CRF regulates pain sensation by enhancement of corticoaccumbal excitatory synaptic transmission

Jun-Li Cao

caojl0310@aliyun.com

Jiangsu Province Key Laboratory of Anesthesiology & Jiangsu Province Key Laboratory of Anesthesia and Analgesia Application Technology, Xuzhou Medical University, Xuzhou 221004, China.

https://orcid.org/0000-0002-8932-4743

Weinan Zhao

Xiao-Yi Wang

Sun-Hui Xia

Yu Ma

He Li

Yumei Yu

Zheng Xu

Jun-Xia Yang

Peng Wu

Hongxing Zhang

Xuzhou Medical University

Hai-Lei Ding

Jiangsu Province Key Laboratory of Anesthesiology & Jiangsu Province Key Laboratory of Anesthesia and Analgesia Application Technology, Xuzhou Medical University, Xuzhou 221004, China.

Article

Keywords:

Posted Date: September 28th, 2023

DOI: https://doi.org/10.21203/rs.3.rs-3137231/v1

Additional Declarations: The authors have declared there is **NO** conflict of interest to disclose

Version of Record: A version of this preprint was published at Molecular Psychiatry on March 7th, 2024. See the published version at https://doi.org/10.1038/s41380-024-02488-7.

Abstract

Both peripheral and central CRF systems have been implicated in regulating pain sensation. However, compared with the peripheral, the mechanisms underlying central CRF system in pain modulation have not yet been elucidated, especially at the neural circuit level. The corticoaccumbal circuit, a structure rich in CRF receptors and CRF-positive neurons, plays an important role in behavioral responses to stressors including nociceptive stimuli. The present study was designed to investigate whether and how CRF signaling in this circuit regulated pain sensation under physiological and pathological pain conditions. Our studies employed the viral tracing and circuit-, and cell-specific electrophysiological methods to label $mPFC^{CRF}$-NAcS circuit and record its neuronal propriety. Combining optogenetic and chemogenetic manipulation, neuropharmacological methods, and behavioral tests, we were able to precisely manipulate this circuit and depicted its role in regulation of pain sensation. The current study found that the CRF signaling in the NAcS, but not NAc core, was necessary and sufficient for the regulation of pain sensation under physiological and pathological pain conditions. This process was involved in the CRF-mediated enhancement of excitatory synaptic transmission in the NAcS. Furthermore, we demonstrated that the $mPFC^{CRF}$ neurons monosynaptically connected with the NAcS neurons. Chronic pain increased the release of CRF into NAcS, and then maintained the persistent NAcS neuronal hyperactivity through enhancement of this monosynaptic excitatory connection, and thus sustained chronic pain behavior. These findings reveal a novel cell- and circuit-based mechanistic link between chronic pain and the $mPFC^{CRF}$→NAcS circuit and provide a potential new therapeutic target for chronic pain.

INTRODUCTION

Corticotropin-releasing factor (CRF), widely expressed in the central nervous system, was initially known as an essential modulator in coordinating physiological responses to stress[1–5]. In recent decades, the role of the central CRF system in the modulation of multiple psychiatric and mental disorders, such as addiction, anxiety, and depression, has received increasing attention [6–8].

Chronic pain is considered to be a persistent and intense stressor [9]. Accumulating evidence suggests that central CRF signaling has been implicated in regulating physiological and pathological pain [10–14]. For instance, in patients with fibromyalgia, pain and depressive symptoms are strongly associated with the CRF concentration in cerebrospinal fluid [12]. Preclinical studies have shown that intracerebroventricular administration of CRF can induce hyperalgesia or analgesia in different animal models [15, 16]. However, the mechanisms underlying the role of central CRF system in pain modulation have yet to be elucidated, especially at the neural circuit level.

The limbic brain, a structure rich in CRF receptors and CRF-positive neurons, is a critical neural network regulating pain and pain-related disorders [17–20]. Embedded within the center of this network is the nucleus accumbens (NAc), a complex neuropeptidergic hub that synthesizes motivation, emotion, learning, cognitive, and sensorimotor information [21–23]. The NAc also plays a vital role in pain regulation and is effective as a source of analgesia [24–27]. Functional magnetic resonance imaging

(fMRI) studies have found characteristic imaging manifestations in the NAc in patients with persistent pain conditions [24, 28, 29]. Deep brain stimulation (DBS) in the NAc has provided sustained pain relief in patients undergoing chronic pain [30]. In preclinical studies, the blockade of glutamate or dopamine (DA) receptors in the NAc has been shown to relieve hyperpathia symptoms [31, 32]. As a neuropeptidergic hub, the NAc contains multiple neuropeptides, including CRF, to modulate local synaptic plasticity, neuronal activity and genetic expression [33–36]. However, depicting the roles and its potential mechanism of these neuropeptides in NAc-related pain regulation still need to be complemented by further research efforts.

CRF signaling in the NAc is involved in multiple biological functions, such as motivation and emotion [37, 38]. For example, CRF in the NAc governs the emotional response to acute stressors via the regulation of dopamine release [39], and can mediate anxiety-like behaviors [40]. A previous study indicated that chronic neuropathic pain induced CRF receptor overexpression in the NAc [41]. In addition, exogenous CRF in the NAc generated a variety of aversive behaviors, such as depression and anxiety [42]. These findings implied the connection between CRF signaling in the NAc and pain information processing, while the underlying mechanism remains unknown.

To address these questions, we used a combination of optogenetics, slice electrophysiology, neuropharmacology, and behavioral tests to examine the role of accumbal CRF signaling in pain regulation and the underlying cellular and synaptic mechanisms. We also performed transsynaptic virus tracing, projection-specific optogenetic and slice recording experiments to examine whether the monosynaptic connections between medial prefrontal cortex (mPFC) CRF-containing neurons and NAc neurons are necessary and sufficient for the regulation of pain sensation. The results revealed a novel cell- and circuit-based mechanistic link between regulation of pain sensation and the CRF signaling in corticoaccumbal circuit.

METHODS AND MATERIALS

Animals

All experiments were reviewed and approved by the Animal Care and Use Committee of Xuzhou Medical University, and performed in accordance with the National Institutes of Health Guidelines and Use of Laboratory Animals and the Committee for Research and Ethical Issues of the International Association for the Study of Pain. Mice were group-housed (maximum five mice per cage) under a 12-h light/dark cycle (light from 8:00 A.M. to 8:00 P.M.), with food and water available ad libitum. The ambient temperature was maintained at 21–22°C with 55% relative humidity. Only C57BL/6 J male mice (8–13 weeks old) of normal weight (22-24g) were used for all studies. All behavioral tests were conducted during the light period, and the investigators were blinded to experimental conditions during testing.

Data analysis and statistics

Prior to further analysis, each dataset was subjected to a normality test using the *Shapiro–Wilk* test. For datasets that were normally distributed, parametric tests of the variance and group differences (paired, unpaired *t* tests, one-way or two-way ANOVA with repeated measures followed by *Bonferroni* post–tests) were used. Otherwise, the non-parametric *Wilcoxon* matched-pairs signed rank test, *Mann Whitney* Rank Sum Test, and the *Kruskal Wallis* One Way ANOVA on ranks with Uncorrected *Dunn's* test were used. Statistical analyses were conducted with GraphPad Prism 7.0 software (GraphPad Software) without specification. All data are shown ± standard error to the mean (SEM). The Detailed descriptions can be found in the figure legends. Statistical significance was set at four levels (*$p < 0.05$, **$p < 0.01$, ***$p < 0.001$, ****$p < 0.0001$).

Detailed information about the materials and methods is described in the supplementary material.

RESULTS

CRF signaling in the NAcS regulates pain

Details on the expression pattern of CRF messenger RNA (mRNA) and protein in the bilateral NAc during the development of chronic pain are still lacking [3, 43–45]. Using a neuropathic pain model of chronic constrictive injury (CCI) of the sciatic nerve, we found a significant increase in CRF protein expression in the contralateral, but not ipsilateral, NAc to the injury site at 3, 7, 14, and 21 days following CCI surgery (Fig. 1A, B), while the level of *Crf* mRNA at these time points in the bilateral NAc did not exhibit any detected changes (Fig. 1C).

The NAc is usually divided into two functionally distinct subregions: the NAc shell (NAcS) and core (NAcC) [46]. Thus, to determine the role and possible difference in CRF signaling in the two subregions in pain regulation, we measured the change in PWTs and PWLs to assess pain sensation in CCI mice after pharmacological inhibition of CRF receptors by injecting a competitive CRF receptor antagonist (-helical CRF, 200 μM, 0.1 μL) into the NAcS or NAcC (Fig. 1D, S1A). Behavioral results showed that intra-NAcS, but not intra-NAcC, -helical CRF injection significantly reversed the established thermal and mechanical hyperalgesia in CCI mice (Fig. 1E, S1B). Repeated injection of -helical CRF into the NAcS, but not into the NAcC, for 5 consecutive days via a pre-implanted cannula produced a prolonged antinociceptive effect, which lasted at least 2 days from the last injection (Fig. 1F, G, S1C, D). In the multiple-injection experiment, behavioral tests were performed eight hours after each injection to exclude the acute anti-nociceptive effect of CRF receptor antagonist (Fig. 1F, S1C). These results suggested that CRF signaling in the NAcS is necessary for regulating the pain sensation underlying the chronic neuropathic pain state.

To investigate whether the activation of CRF signaling in the NAc in naïve mice is sufficient to regulate pain sensation, exogenous CRF (0.1 μL) was injected into the NAcS or NAcC to activate CRF signaling before behavioral tests. The results showed that intra-NAcS CRF injection significantly decreased the PWLs and PWTs in the paw contralateral to the injection site in naïve mice, and this effect was observed after the 50 nM, but not the 200 nm and 1000 nm, CRF injection (Fig. 1H), while this decrement was

absent after the intra-NAcC injection (Fig. S1E). A stable and high level of CRF protein expression in the NAc after CCI surgery was observed. Thus, we want to know whether continuously activated CRF signaling in the NAcS through repeated injection of CRF (50n M, once per day for 5 days) is sufficient to induce a persistent pain state. The current results indicated that this repeated activation produced a prolonged painful effect and this effect lasted at least 2 days from the last injection (Fig. 1I, J). Repeated injection of CRF into the NAcC did not affect pain sensation in naïve mice (Fig. S1F, G). These findings demonstrated that the stable and high level of CRF protein in the NAcS after CCI surgery played an important role in pain sensation regulation and the establishment of persistent pain conditions.

CRF increases neuronal excitability in the NAcS by enhancing excitatory synaptic transmission

Next, we asked how CRF signaling in the NAcS regulates pain sensation and participates in the development of chronic neuropathic pain. In the CNS, the functional changes were mainly dependent on alterations in neuronal excitability [47, 48]. Using the whole-cell patch clamp recordings in acutely isolated NAc slices (Fig. 2A, S2A) from sham and CCI mice, we measured neuronal excitability by the number of evoked action potentials by depolarizing current injections (eAPs). Compared to sham mice, CCI mice showed a significant increase in the number of eAps, suggesting an increase in neuronal excitability in the NAcS but not in the NAcC (Fig. 2. B top and C left; Fig. S2. B, C). Interestingly, the resting membrane potential (RMP) and rheobase current in NAcS neurons were unaffected by CCI surgery (Fig. S3A). The changes in both synaptic transmission and neuronal intrinsic properties can affect neuronal excitability [49]. Thus, we then examined intrinsic neuronal excitability, which was defined as its excitability in the absence of synaptic inputs by blocking both inhibitory and excitatory synaptic transmission [by blocking $GABA_A$ receptors ($GABA_A$Rs) with 100 μM picrotoxin, AMPA (-amino-3-hydroxy-5-methyl-4-isoxazolepropionic acid) receptors (AMPARs) with 10 μM NBQX, and NMDA (N-methyl-D-aspartate) receptors (NMDARs) with 50 μM D-AP5]. We found that the intrinsic neuronal excitability in the NAcS was not significantly different between the CCI and sham groups (Fig. 2. B bottom and C right; Fig. S3B). These data indicated that the increase in NAcS neuronal excitability in CCI mice is due to alterations of synaptic transmission.

Next, we want to explore the contribution of CRF signaling to the NAcS neuronal excitability. In isolated NAc slices from CCI mice, perfusion with -helical CRF (200 μM), but not its control Acsf, significantly decreased the number of eAPs (Fig. 2D), suggesting CRF signaling made a contribution to the increased neuronal excitability in CCI mice. Furthermore, in isolated NAc slices from naïve mice, CRF (50 nM) perfusion increased the number of eAPs (Fig. 2E). Neither -helical CRF nor CRF perfusion affected the RMP or rheobase current in NAcS neurons (Fig. S4A, B). Next, we repeated the above experiments with the blockade of inhibitory and excitatory synaptic transmission. We found that, in the absence of synaptic transmission, neither -helical CRF perfusion in CCI mice nor CRF perfusion in naïve mice influenced the excitability of NAcS neurons (Fig. 2F, G; Fig S4C, D).

The above findings suggested that the increase of NAcS neuronal excitability induced by CCI injury or exogenous CRF in naïve mice might be due to changes in synaptic transmission. Thus, we next examined changes in inhibitory and excitatory synaptic transmission in NAcS neurons in CCI mice. We found that the frequency and amplitudes of spontaneous inhibitory postsynaptic currents (sIPSCs) did not differ between CCI and sham mice (Fig. 2H, I). However, the frequency of spontaneous excitatory postsynaptic currents (sEPSCs) of the NAcS neurons is significantly increased in CCI mice compared with sham group, while its amplitude is unchanged (Fig. 2J, K). Furthermore, -helical CRF (200 μM) perfusion decreased the frequency, but not amplitude, of sEPSCs in CCI mice (Fig. 2L, M). Consistently, CRF (50 nM) perfusion in NAc slice from sham group mice increased its frequency, but not amplitude, of sEPSCs (Fig. 2N, O). These results demonstrated that CRF signaling increased NAcS neuronal excitability through enhanced excitatory presynaptic transmission.

CRF-containing mPFC neurons innervate the NAcS for the maintenance of chronic neuropathic pain

In general, the level of mRNA is determined by local transcription, while the protein level is determined by both local synthesis and projection-release. In the present study, the levels of CRF mRNA and protein in the NAc were inconsistently changed under chronic neuropathic pain (Fig. 1C), suggesting that the increase in CRF protein in CCI mice may be due to the release of CRF from presynaptic terminals rather than local synthesis in the NAcS. On the other hand, approximately 95% of neurons in the NAc are GABAergic medium spiny neurons, which cannot induce an increase in sEPSCs in CCI mice [50]. Therefore, we speculated that the increase in CRF protein and sEPSCs in the NAcS is due to afferents from excitatory neurons outside the NAcS. To test this hypothesis, the retrograde virus AAV-CRF-eYFP was injected into the NAcS 21 days before, and then the whole-brain examination of eYFP expression was performed to trace the NAcS-projection CRF positive neurons (Fig. S5A). Consistent with a previous report [51], among multiple pain-related regions, we found that CRF-containing neurons in the prelimbic cortex and infralimbic cortex (two important neuroanatomical subregions of the mPFC [52]) preferentially innervated the NAcS (Fig. S5B, C). Immunofluorescences staining confirmed that over 98% of these eYFP positive neurons in mPFC express CRF protein (Fig. S5D, E). In addition, 70% of NAcS-projecting CRF-containing neurons in the mPFC (called $mPFC^{CRF}$→NAcS neurons) were co-labeled with CaMKIIα, a widely used marker of excitatory neurons (Fig. S5F, G), suggesting that these neurons were mainly excitatory pyramidal neurons. These findings led us to hypothesize that the $mPFC^{CRF}$→NAcS circuit participates in the maintenance of chronic neuropathic pain.

To examine the potential role of the $mPFC^{CRF}$→NAcS circuit in chronic neuropathic pain, we first detected neuronal activities through double immunofluorescence staining for c-Fos and eYFP, and the $mPFC^{CRF}$→NAcS neurons were labeled with eYFP in the mPFC 7 days after CCI surgery (Fig. 3A). Compared with sham mice, CCI mice showed a significant increased total numbers and percentages of c-Fos expression in $mPFC^{CRF}$→NAcS neurons (Fig. 3B, C). Projection-specific slice recordings also revealed that CCI mice displayed higher excitability in $mPFC^{CRF}$→NAcS neurons than sham mice as evidenced by

higher numbers of eAPs and lower rheobase current (Fig. 3D-F). Furthermore, we found that both the mRNA and protein levels of CRF in the mPFC exhibited significant increases in CCI mice (Fig. 3G, H). These results suggested that chronic neuropathic pain was accompanied by hyperactivity of the $mPFC^{CRF}$→NAcS circuit.

To further evaluate the necessity of the $mPFC^{CRF}$→NAcS circuit in mediating chronic neuropathic pain, we injected a retrograde AAV virus expressing Cre recombinase (AAV2/R-CRF-Cre) into the NAcS, and an AAV vector expressing Cre-dependent halorhodopsin (AAV-DIO-NpHR-eYFP) into the mPFC to express NpHR selectively in $mPFC^{CRF}$→NAcS neurons (Fig. 3I, J). Immunofluorescence staining confirmed the expression of eYFP in $mPFC^{CRF}$→NAcS neurons and their axon terminals in the NAcS, and further electrophysiological recordings validated that the activity of the $mPFC^{CRF}$→NAcS neurons was reliably inhibited by optical stimulation (Fig. 3K). The behavioral results showed that acute chemogenetic/optogenetic (589 nm yellow laser, 10 ms pulse, 7 mW intensity, 7 s duration) inhibition of the $mPFC^{CRF}$→NAcS circuit reversed the established hyperalgesia in CCI mice (Fig. 3L, S6A-C), whereas this inhibition did not change basal pain thresholds in sham mice (Fig. S6D, S7A, B). Furthermore, we found that repeated chemogenetic/optogenetic inhibition of the $mPFC^{CRF}$→NAcS circuit (1 h per day, for 7 consecutive days) produced a prolonged antinociceptive effect, which lasted at least 2 days from the last inhibition (Fig. 3M, N, S6E-G). These data demonstrated that chronic neuropathic pain activated the $mPFC^{CRF}$→NAcS circuit, which increased the release of CRF into the NAcS to maintain the chronic pain state through the alteration of neuronal excitability.

The sufficient role of the $mPFC^{CRF}$→NAcS circuit in regulating pain

To examine the sufficient role of the $mPFC^{CRF}$→NAcS circuit in pain regulation, we injected an AAV2/R-CRF-Cre virus into the NAcS and a Cre-dependent virus of channelrodopsin2 (ChR2)-mCherry into the mPFC to express ChR2 in the $mPFC^{CRF}$→NAcS circuit before pain behavioral tests (Fig. 4A, B). Electrophysiological recordings further validated its functional effectiveness, as blue pulses reliably elicited precisely timed action potentials in mCherry-positive neurons in the mPFC (Fig. 4C). We found that transient optogenetic activation of the $mPFC^{CRF}$→NAcS circuit (473 nm blue laser, 5 ms pulse, 7 mW intensity, 100 ms interval, 1h duration) did not affect the PWTs or PWLs in naïve mice (Fig. 4D). This effect was also confirmed by chemogenetic activation with a single CNO (1 mg/kg) injection in naïve mice (Fig. S8A, B). A possible explanation for this finding is that brief activation of the $mPFC^{CRF}$→NAcS circuit did not induce a sufficient increase in CRF protein levels in the NAcS.

Thus, we next detected whether repeated activation of the $mPFC^{CRF}$→NAcS circuit could mimic the pathological process of chronic neuropathic pain. We optogenetically activated the $mPFC^{CRF}$→NAcS circuit 1 h per day for 5 consecutive days, and we performed pain behavioral tests and NAc tissues extraction for western blotting 8 hours after the end of stimulation (Fig. 4E). The results showed that

repeated activation significantly increased the level of CRF protein in the NAc (Fig. 4F, G) and evoked prolonged hyperalgesia in naïve mice, which lasted 2 days from the last activation (Fig. 4H).

To determine whether this hyperalgesia induced by the repeated activation of the mPFC^{CRF}→NAcS circuit was mediated by CRF signaling, we injected a retrograde AAV-CRF-Cre virus into the NAcS and a Cre-dependent AAV-hM3Dq-ChR2-mCherry virus into the mPFC for chemogenetic activation of this circuit, and we implanted the cannula into the NAcS 14 days for microinjection of CRF receptor antagonist before behavioral tests (Fig. 4I, J). Viral function was confirmed by cell-attached recording in the mPFC (Fig. 4K). We found that the inhibition of CRF receptors with 200 μM -helical CRF (0.1 μL) before each activation abolished the hyperalgesia induced by the repeated activation of the mPFC^{CRF}→NAcS circuit (Fig. 4L). Collectively, these data suggested that the repeated activation of the mPFC^{CRF}→NAcS circuit resulted in the increased release of CRF in the NAc, which was sufficient to induce chronic neuropathic pain-like hyperalgesia.

Identifying monosynaptic connection in the mPFC→NAcS circuit and its functional alteration in chronic neuropathic pain

To disentangle the precise mechanisms of the mPFC^{CRF}→NAcS circuit underlying pain regulation, we used an optogenetic approach and electrophysiological recording (Fig. 5A, B). We found that optogenetic activation (473 nm blue laser, 5 ms pulse) of terminals of the mPFC^{CRF}→NAcS circuit induced large light-evoked excitatory postsynaptic currents (leEPSCs) in 42.9% of NAcS neurons. Pharmacological experiments demonstrated that leEPSCs were completely abolished by the application of the AMPA receptor antagonist NBQX (Fig. 5C), indicating that synaptic responses are mediated by AMPA receptors. To eliminate polysynaptic transmission relying on action potential propagation, tetrodotoxin (TTX, 1 μM) was added to the bath solution at least 5 minutes before the start of recording. These findings suggested that these NAcS neurons which responded to the optical stimulation received the monosynaptic excitatory inputs from mPFC^{CRF}→NAcS neurons.

Next, to explore the functional changes in these monosynaptic connections in CCI mice, two consecutive optogenetic stimulations (473 nm blue laser, 5 ms pulse, 50 ms interval) were used to obtain the paired-pulse ratio (PPR) in these NAcS neurons. We found a decrease in the PPR (Fig. 5D) and the unchanged in the AMPAR/NMDAR amplitude ratio in CCI mice (Fig. S9A-B), indicating an increased probability of presynaptic release of the mPFC^{CRF}→NAcS circuit under chronic pain conditions rather than a change in postsynaptic strength. Furthermore, the application of CRF increased the PPR in sham mice, and the application of -helical CRF decreased the PPR in CCI mice (Fig. 5E), confirming that the increased synaptic efficacy in the mPFC^{CRF}→NAcS circuit was mediated by CRF signaling.

We next employed cell-type-specific WGA-mediated transsynaptic tracings to selectively label NAcS-receiving neurons innervated by mPFC CRF-containing neurons (called NAcS-receiving neurons), and then we examined their functional changes via electrophysiological recordings. An AAV vector expressing the

transsynaptic tracer wheat germ agglutinin (WGA) fused to Cre-recombinase (AAV-CRF-WGA-Cre) and a cre-dependent viral vector expressing mCherry (AAV-DIO-mCherry) were injected into the mPFC and NAcS, respectively (Fig. 5F). Notably, although WGA-mediated transsynaptic transport is bidirectional [53], a previous study and our data show that few neurons within the NAc directly innervate the mPFC (Fig. S10 A-C) [54], which means that this strategy in the $mPFC^{CRF}$→NAcS circuit can unidirectionally target the receiving NAcS neurons. The results showed that the number of eAPs was significantly increased, the rheobase current was decreased, and the RMP was not affected in these mCherry-labeled NAcS-receiving neurons in CCI mice (Fig. 5G; Fig. S11A-B). These findings suggested that the increased neuronal excitability in NAcS-receiving neurons was accompanied by a chronic neuropathic pain state. Furthermore, we found that -helical CRF (200 μM) perfusion inhibited neuronal excitability in NAcS-receiving neurons, as evidenced by fewer eAPs and an increased rheobase current in CCI mice (Fig. 5I), and CRF (50 nM) perfusion enhanced neuronal excitability in naïve mice (Fig. 5J). Neither -helical CRF nor CRF perfusion affected RMP in NAcS-receiving neurons (Fig. S12A-B).

Consistent with the overall changes in the neurons of the NAcS, chronic pain-induced changes in sIPSCs in NAcS-receiving neurons were also not detected in CCI mice (Fig. S13A-C), while an increase in the frequency, but not amplitude, of sEPSCs in NAcS-receiving neurons was observed in CCI mice (Fig. 5H). Moreover, perfusion with α-helical CRF abolished the above increase in CCI mice, and CRF perfusion increased the sEPSCs frequency in NAcS-receiving neurons in sham mice (Fig. 5K, L).

The role of NAcS-receiving neurons in chronic pain

Although we demonstrated the monosynaptic connections between NAcS neurons and mPFC CRF-containing neurons and their functional changes under chronic neuropathic pain conditions, the role of NAcS-receiving neurons in the regulation of pain behaviors was still unclear. To answer this question, we injected the AAV-CRF-WGA-Cre virus into the mPFC and AAV-DIO-hM4D(Gi)-mCherry into the NAcS, and then we could specifically inhibit the activity of NAcS-receiving neurons via intraperitoneal injection of CNO (Fig. 6A, B). The viral function was confirmed by cell-attached recording in the NAcS. (Fig. 6C). Behavioral results showed that chemogenetic inhibition of these NAcS-receiving neurons did not change the basal pain thresholds in naïve mice (Fig. 6D) and reversed the established hyperalgesia in CCI mice compared to the virus control mice (Fig. 6E).

Next, we wanted to know whether repeated inactivation of activity in these NAcS-receiving neurons could produce a prolonged antinociceptive effect in CCI mice. We performed the same repeated CNO injection strategy and behavioral tests as previous experiments (Fig. 6F). Interestingly, unlike the prolonged antinociceptive effect observed with repeated inhibition of the $mPFC^{CRF}$→NAcS circuit or CRF signaling in the NAcS, this repeated inactivation for 7 consecutive days did not produce any detectable changes of thermal and mechanical threshold in CCI mice (Fig. 6G). These data suggested that the hyperactivity of NAcS neurons innervated by the $mPFC^{CRF}$→NAcS circuit is necessary for the maintenance of chronic neuropathic pain, and persistent CRF-mediated enhancement of excitatory synaptic input is also necessary for maintaining the hyperactivity of these NAcS-receiving neurons.

DISCUSSION

Our current results demonstrated that CRF signaling in the NAcS is necessary and sufficient for the regulation of pain sensation under both physiological and pathological pain conditions, which was mediated by the enhancement of excitatory synaptic transmission in the $mPFC^{CRF}$→NAcS circuit (Fig. 6H). These findings reveal a novel cell- and circuit-based mechanistic link between chronic pain and the $mPFC^{CRF}$→NAcS circuit and provide potential therapeutic interventions for chronic pain by targeting the CRF neuronal circuit.

In recent decades, an increasing number of studies have suggested the role of extrahypothalamic CRF signaling including some brain regions such as the amygdala, hypothalamus, and periaqueductal gray in the regulation of pain sensation and pain-related affective behaviors [11–14, 55–62]. However, a comprehensive understanding of the brain mechanisms underlying CRF-mediated pain regulation is still lacking. We found that CCI-induced chronic neuropathic pain was accompanied with a persistent high CRF protein level in the NAc, which was in agreement with a previous study showing that CCI surgery evoked the overexpression of CRF receptors in the NAc [41]. Furthermore, we also demonstrated that CRF signaling in the NAcS was necessary and sufficient for the regulation of pain sensation under both physiological and pathological pain conditions. However, only low concentrations of CRF (50 nM) caused hyperpathia in naïve mice. In previous studies, a narrow effective dose range of CRF to evoke hyperalgesia/analgesia in the central nervous system was also observed [13, 16, 63]. CRF shows the highest affinity for binding to CRF receptor type (CRFR1) but may also bind to CRF receptor type (CRFR2) at very high concentrations [64, 65]. The action of activating the two receptors is thought to be antagonistic in previous pharmacological experiments [2, 66]. Thus, the concentration-dependent effect in our experiments may be attributed to the distinct constitution of two receptor subtypes activated by the different concentrations of CRF[49, 63, 67].

Interestingly, we found that repeated pharmacological activation of CRF receptors in the NAcS for 5 days resulted in chronic pain-like nociceptive responses that persisted for several days after the termination of pharmacological activation, and prolonged inhibition of CRF receptors induced persistent pain relief. Post-injury hyperpathia has been attributed to the sensitization and increased excitability of peripheral nociceptors or central neurons, with neuropeptides playing important modulatory roles throughout the process [68–73]. Our results suggest that the enhanced CRF signaling in NAc is a critical contributor to pain sensation regulation under physiological conditions and to the development of chronic neuropathic pain.

Growing evidence implied that the subregions of the NAc play distinct roles in processing pain information [28, 74]. In agreement with this view, we found that CRF signaling in the NAcS, but not in the NAcC, is involved in pain regulation. Similar subregion-specific effect in NAc has also been observed in the CRF-mediated oral motor activity [74]. Differential distributions of CRF receptors and CRF fiber innervating the NAcS or NAcC may account for these functional heterogeneities of NAc CRF signaling [75–77].

Several lines of evidence have indicated a link between enhanced neural activity in the NAc and painful experiences in humans and rodents [28, 41, 68, 69]. Consistently, the present study also indicated that neuronal activity and excitability in the NAcS, but not in the NAcC, were increased in CCI mice. Neuronal activity or excitability is affected by local intrinsic molecular mechanisms and presynaptic inputs from the innervating neurons [78, 79]. The transmission of glutamate in NAc has been involved in the neuronal activity and function [80–82]. The present study found that 1) the frequency, but not the amplitude, of sEPSC in NAcS neurons was increased in CCI mice and 2) the CCI-induced increase in excitability in NAcS neurons was reversed by blocking of excitatory synaptic transmission. The pain-related changes of excitatory input into NAc were also observed in several previous experiments [83, 84], while the mechanisms underlying these changes remains unclear. Our current data revealed that exogenous CRF enhances the excitatory synaptic transmission and inhibition of accumbal CRF signaling decreased presynaptic glutamate release. Combined with the previous researches, which revealed the crucial role of CRF in the modulation of presynaptic release [39, 42, 85], current results suggest that CRF-mediated enhancement of excitatory synaptic transmission accounted for neuronal hyperexcitability in NAcS neurons in CCI mice.

In line with the findings from previous whole-brain mapping studies in mice [51], our virally mediated retrograde tracing study determined that NAcS neurons were densely innervated by CRF-containing neurons in the mPFC. Animal and human study findings have implicated the neuronal connection between the mPFC and the NAc in the development of chronic pain [86–88]. However, the detailed mechanisms of this pain-related association reinforcement are still lacking. Our results indicate that the $mPFC^{CRF}$→NAcS circuit was activated following CCI surgery, as evidenced by increased c-Fos expression and neuronal excitability in NAcS-projecting mPFC CRF-containing neurons. Real-time optogenetic inhibition of the $mPFC^{CRF}$→NAcS circuit relieved hyperalgesia in CCI mice. In line with our pharmacological results, previous study which preferentially activating the NAcC-projecting mPFC CRF-positive neurons did not observed the influence of pain sensation [41]. These findings suggested that the persistent activation of the $mPFC^{CRF}$→NAcS circuit is essential for the maintenance of chronic pain.

Consistent with pharmacological inhibition of CRF signaling in the NAcS, repeated optogenetic inhibition of this circuit produced significant pain sensation relief in CCI mice, and this effect lasted for days after the termination of optical stimulation. These results indicate that the $mPFC^{CRF}$→NAcS circuit also governs the development of neuropathic pain. Prolonged inhibition of $mPFC^{CRF}$-NAcS circuit may reduce the release of CRF, relieve CRF-mediated excitation in the $mPFC^{CRF}$-NAcS circuit and prevent the hyperexcitability of NAcS neurons induced by CCI surgery. The result that acute optogenetic activation of $mPFC^{CRF}$→NAcS circuit did not affect the paw-withdrawal response in naïve mice is in sharp contrast to the effect of pharmacological manipulation. One possibility for the discrepancy between the result of optogenetic and pharmacological activation may be that the released CRF which is evoked by transitory activation is not sufficient for inducing hyperpathia, as CRF is stored in large dense core granules [89] and likely released by a prolonged period of activation [90, 91]. This hypothesis is supported by the following

results that repeated activation of the mPFC^{CRF}→NAcS circuit induced a significant chronic pain-like response, which was accompanied by an increase in CRF protein levels in the NAc.

Interestingly, repeated inhibition of the mPFC^{CRF}→NAcS circuit or its NAcS-receiving neurons produced different effects on the regulation of pain sensation. Unlike the prolonged antinociceptive effect seen after the inhibition of the mPFC^{CRF}→NAcS circuit, the same manipulation on NAcS neurons innervated by the mPFC CRF-containing neurons induced only a transient antinociceptive effect. The NAc is known as one pivotal relay station for pain signaling as it receives innervation from both the prefrontal cortex and limbic regions, and projects forward to motor regions [25, 30]. Our findings suggested that 1) the regulation of pain sensation by NAcS-receiving neurons requires persistent inputs from the mPFC^{CRF}→NAcS circuit; and 2) targeting the mPFC^{CRF}→NAcS circuit may be more effective than interfering only with its receiving neurons.

In conclusion, the present findings revealed a novel cellular, synaptic and circuitry mechanism for pain regulation by central CRF signaling, and targeting CRF signaling in the corticoaccumbal circuit may be a potential therapeutic avenue for chronic pain.

Declarations

Acknowledgements

The present study was supported by the National Key R&D Program of China—the Sci-Tech Innovation 2030 Major Project (2021ZD0203100), the National Natural Science Foundation of China (82130033, 82293641, 31970937, 82271255, 82101315 and 82271263); Jiangsu Province Innovative

and Entrepreneurial Team Program, the Key Project of Nature Science Foundation of Jiangsu Education Department (22KJA320006); the Innovation and Entrepreneurship Program of Xuzhou Medical University (2021CXFUZX002), China Postdoctoral Science Foundation (2022M710771 and 2022M722676), the Postgraduate Research & Practice Innovation Program of Jiangsu Province (KYCX21_2704).

The authors thank Li Yang, Dong-Yu Zhou, Wei Zheng and Prof. Cheng Xiao

for technical supports.

Conflict of Interest

All authors reported no biomedical financial interests or potential conflicts of interest.

Supplementary information is available at MP's website.

References

1. Walsh JJ, Friedman AK, Sun H, Heller EA, Ku SM, Juarez B *et al.* Stress and CRF gate neural activation of BDNF in the mesolimbic reward pathway. *Nat Neurosci* 2014; **17**(1)**:** 27-29.
2. Bale TL, Vale WW. CRF and CRF receptors: role in stress responsivity and other behaviors. *Annu Rev Pharmacol Toxicol* 2004; **44:** 525-557.
3. Henckens MJ, Deussing JM, Chen A. Region-specific roles of the corticotropin-releasing factor-urocortin system in stress. *Nat Rev Neurosci* 2016; **17**(10)**:** 636-651.
4. Lv Y, Chen P, Shan QH, Qin XY, Qi XH, Zhou JN. Regulation of Cued Fear Expression via Corticotropin-Releasing-Factor Neurons in the Ventral Anteromedial Thalamic Nucleus. *Neurosci Bull* 2021; **37**(2)**:** 217-228.
5. Engelke DS, Zhang XO, O'Malley JJ, Fernandez-Leon JA, Li S, Kirouac GJ *et al.* A hypothalamic-thalamostriatal circuit that controls approach-avoidance conflict in rats. *Nat Commun* 2021; **12**(1)**:** 2517.
6. Koob GF. The role of CRF and CRF-related peptides in the dark side of addiction. *Brain Res* 2010; **1314:** 3-14.
7. Binder EB, Nemeroff CB. The CRF system, stress, depression and anxiety-insights from human genetic studies. *Mol Psychiatry* 2010; **15**(6)**:** 574-588.
8. Chen P, Lou S, Huang ZH, Wang Z, Shan QH, Wang Y *et al.* Prefrontal Cortex Corticotropin-Releasing Factor Neurons Control Behavioral Style Selection under Challenging Situations. *Neuron* 2020; **106**(2)**:** 301-315.e307.
9. Abdallah CG, Geha P. Chronic Pain and Chronic Stress: Two Sides of the Same Coin? *Chronic Stress (Thousand Oaks)* 2017; **1**.
10. Yu W, Caira CM, Del RRSN, Moseley GA, Kash TL. Corticotropin-releasing factor neurons in the bed nucleus of the stria terminalis exhibit sex-specific pain encoding in mice. *Sci Rep* 2021; **11**(1)**:** 12500.
11. Bourbia N, Ansah OB, Pertovaara A. Corticotropin-releasing factor in the rat amygdala differentially influences sensory-discriminative and emotional-like pain response in peripheral neuropathy. *J Pain* 2010; **11**(12)**:** 1461-1471.
12. McLean SA, Williams DA, Stein PK, Harris RE, Lyden AK, Whalen G *et al.* Cerebrospinal fluid corticotropin-releasing factor concentration is associated with pain but not fatigue symptoms in patients with fibromyalgia. *Neuropsychopharmacology* 2006; **31**(12)**:** 2776-2782.
13. Larauche M, Moussaoui N, Biraud M, Bae WK, Duboc H, Million M *et al.* Brain corticotropin-releasing factor signaling: Involvement in acute stress-induced visceral analgesia in male rats. *Neurogastroenterol Motil* 2019; **31**(2)**:** e13489.
14. Lariviere WR, Melzack R. The role of corticotropin-releasing factor in pain and analgesia. *Pain* 2000; **84**(1)**:** 1-12.
15. Vit JP, Clauw DJ, Moallem T, Boudah A, Ohara PT, Jasmin L. Analgesia and hyperalgesia from CRF receptor modulation in the central nervous system of Fischer and Lewis rats. *Pain* 2006; **121**(3)**:** 241-260.

16. Williams DW, Jr., Lipton JM, Giesecke AH, Jr. Influence of centrally administered peptides on ear withdrawal from heat in the rabbit. *Peptides* 1986; **7**(6)**:** 1095-1100.
17. Thompson JM, Neugebauer V. Cortico-limbic pain mechanisms. *Neurosci Lett* 2019; **702:** 15-23.
18. Zhu X, Zhou W, Jin Y, Tang H, Cao P, Mao Y *et al.* A Central Amygdala Input to the Parafascicular Nucleus Controls Comorbid Pain in Depression. *Cell Rep* 2019; **29**(12)**:** 3847-3858.e3845.
19. Zhou W, Jin Y, Meng Q, Zhu X, Bai T, Tian Y *et al.* A neural circuit for comorbid depressive symptoms in chronic pain. *Nat Neurosci* 2019; **22**(10)**:** 1649-1658.
20. Takahashi D, Asaoka Y, Kimura K, Hara R, Arakaki S, Sakasai K *et al.* Tonic Suppression of the Mesolimbic Dopaminergic System by Enhanced Corticotropin-Releasing Factor Signaling Within the Bed Nucleus of the Stria Terminalis in Chronic Pain Model Rats. *J Neurosci* 2019; **39**(42)**:** 8376-8385.
21. Castro DC, Bruchas MR. A Motivational and Neuropeptidergic Hub: Anatomical and Functional Diversity within the Nucleus Accumbens Shell. *Neuron* 2019; **102**(3)**:** 529-552.
22. Liu D, Tang QQ, Yin C, Song Y, Liu Y, Yang JX *et al.* Brain-derived neurotrophic factor-mediated projection-specific regulation of depressive-like and nociceptive behaviors in the mesolimbic reward circuitry. *Pain* 2018; **159**(1)**:** 175.
23. An K, Zhao H, Miao Y, Xu Q, Li YF, Ma YQ *et al.* A circadian rhythm-gated subcortical pathway for nighttime-light-induced depressive-like behaviors in mice. *Nat Neurosci* 2020; **23**(7)**:** 869-880.
24. Baliki MN, Geha PY, Fields HL, Apkarian AV. Predicting value of pain and analgesia: nucleus accumbens response to noxious stimuli changes in the presence of chronic pain. *Neuron* 2010; **66**(1)**:** 149-160.
25. Harris HN, Peng YB. Evidence and explanation for the involvement of the nucleus accumbens in pain processing. *Neural Regen Res* 2020; **15**(4)**:** 597-605.
26. Guo F, Du Y, Qu FH, Lin SD, Chen Z, Zhang SH. Dissecting the Neural Circuitry for Pain Modulation and Chronic Pain: Insights from Optogenetics. *Neurosci Bull* 2022; **38**(4)**:** 440-452.
27. Zhang H, Qian YL, Li C, Liu D, Wang L, Wang XY *et al.* Brain-Derived Neurotrophic Factor in the Mesolimbic Reward Circuitry Mediates Nociception in Chronic Neuropathic Pain. *Biol Psychiatry* 2017; **82**(8)**:** 608-618.
28. Makary MM, Polosecki P, Cecchi GA, DeAraujo IE, Barron DS, Constable TR *et al.* Loss of nucleus accumbens low-frequency fluctuations is a signature of chronic pain. *Proc Natl Acad Sci U S A* 2020; **117**(18)**:** 10015-10023.
29. Seminowicz DA, Remeniuk B, Krimmel SR, Smith MT, Barrett FS, Wulff AB *et al.* Pain-related nucleus accumbens function: modulation by reward and sleep disruption. *Pain* 2019; **160**(5)**:** 1196-1207.
30. Mallory GW, Abulseoud O, Hwang SC, Gorman DA, Stead SM, Klassen BT *et al.* The nucleus accumbens as a potential target for central poststroke pain. *Mayo Clinic proceedings* 2012; **87**(10)**:** 1025-1031.
31. Jing PB, Chen XH, Lu HJ, Gao YJ, Wu XB. Enhanced function of NR2C/2D-containing NMDA receptor in the nucleus accumbens contributes to peripheral nerve injury-induced neuropathic pain and

depression in mice. *Mol Pain* 2022; **18:** 17448069211053255.

32. Faramarzi G, Zendehdel M, Haghparast A. D1- and D2-like dopamine receptors within the nucleus accumbens contribute to stress-induced analgesia in formalin-related pain behaviours in rats. *Eur J Pain* 2016; **20**(9)**:** 1423-1432.
33. Schank JR, Nelson BS, Damadzic R, Tapocik JD, Yao M, King CE *et al.* Neurokinin-1 receptor antagonism attenuates neuronal activity triggered by stress-induced reinstatement of alcohol seeking. *Neuropharmacology* 2015; **99:** 106-114.
34. Smith NK, Kondev V, Hunt TR, Grueter BA. Neuropeptide Y modulates excitatory synaptic transmission and promotes social behavior in the mouse nucleus accumbens. *Neuropharmacology* 2022; **217:** 109201.
35. Morales-Mulia S, Magdaleno-Madrigal VM, Nicolini H, Genis-Mendoza A, Morales-Mulia M. Orexin-A up-regulates dopamine D2 receptor and mRNA in the nucleus accumbens Shell. *Mol Biol Rep* 2020; **47**(12)**:** 9689-9697.
36. Xia SH, Yu J, Huang X, Sesack SR, Huang YH, Schlüter OM *et al.* Cortical and Thalamic Interaction with Amygdala-to-Accumbens Synapses. *J Neurosci* 2020; **40**(37)**:** 7119-7132.
37. Baumgartner HM, Schulkin J, Berridge KC. Activating Corticotropin-Releasing Factor Systems in the Nucleus Accumbens, Amygdala, and Bed Nucleus of Stria Terminalis: Incentive Motivation or Aversive Motivation? *Biol Psychiatry* 2021; **89**(12)**:** 1162-1175.
38. Marcinkiewcz CA, Prado MM, Isaac SK, Marshall A, Rylkova D, Bruijnzeel AW. Corticotropin-releasing factor within the central nucleus of the amygdala and the nucleus accumbens shell mediates the negative affective state of nicotine withdrawal in rats. *Neuropsychopharmacology* 2009; **34**(7)**:** 1743-1752.
39. Lemos JC, Wanat MJ, Smith JS, Reyes BA, Hollon NG, Van Bockstaele EJ *et al.* Severe stress switches CRF action in the nucleus accumbens from appetitive to aversive. *Nature* 2012; **490**(7420)**:** 402-406.
40. Novoa J, Rivero CJ, Pérez-Cardona EU, Freire-Arvelo JA, Zegers J, Yarur HE *et al.* Social isolation of adolescent male rats increases anxiety and K(+) -induced dopamine release in the nucleus accumbens: Role of CRF-R1. *Eur J Neurosci* 2021; **54**(3)**:** 4888-4905.
41. Kai Y, Li Y, Sun T, Yin W, Mao Y, Li J *et al.* A medial prefrontal cortex-nucleus acumens corticotropin-releasing factor circuitry for neuropathic pain-increased susceptibility to opioid reward. *Transl Psychiatry* 2018; **8**(1)**:** 100.
42. Chen YW, Rada PV, Bützler BP, Leibowitz SF, Hoebel BG. Corticotropin-releasing factor in the nucleus accumbens shell induces swim depression, anxiety, and anhedonia along with changes in local dopamine/acetylcholine balance. *Neuroscience* 2012; **206:** 155-166.
43. Watanabe M, Narita M. Brain Reward Circuit and Pain. *Adv Exp Med Biol* 2018; **1099:** 201-210.
44. Serafini RA, Pryce KD, Zachariou V. The Mesolimbic Dopamine System in Chronic Pain and Associated Affective Comorbidities. *Biol Psychiatry* 2020; **87**(1)**:** 64-73.

45. Elman I, Borsook D. Common Brain Mechanisms of Chronic Pain and Addiction. *Neuron* 2016; **89**(1)**:** 11-36.
46. Ambroggi F, Ghazizadeh A, Nicola SM, Fields HL. Roles of nucleus accumbens core and shell in incentive-cue responding and behavioral inhibition. *J Neurosci* 2011; **31**(18)**:** 6820-6830.
47. Lisman J, Cooper K, Sehgal M, Silva AJ. Memory formation depends on both synapse-specific modifications of synaptic strength and cell-specific increases in excitability. *Nat Neurosci* 2018; **21**(3)**:** 309-314.
48. Bradley C, Nydam AS, Dux PE, Mattingley JB. State-dependent effects of neural stimulation on brain function and cognition. *Nat Rev Neurosci* 2022; **23**(8)**:** 459-475.
49. Authement ME, Langlois LD, Shepard RD, Browne CA, Lucki I, Kassis H *et al.* A role for corticotropin-releasing factor signaling in the lateral habenula and its modulation by early-life stress. *Science signaling* 2018; **11**(520).
50. Robison AJ, Nestler EJ. Transcriptional and epigenetic mechanisms of addiction. *Nat Rev Neurosci* 2011; **12**(11)**:** 623-637.
51. Itoga CA, Chen Y, Fateri C, Echeverry PA, Lai JM, Delgado J *et al.* New viral-genetic mapping uncovers an enrichment of corticotropin-releasing hormone-expressing neuronal inputs to the nucleus accumbens from stress-related brain regions. *J Comp Neurol* 2019; **527**(15)**:** 2474-2487.
52. Heidbreder CA, Groenewegen HJ. The medial prefrontal cortex in the rat: evidence for a dorso-ventral distinction based upon functional and anatomical characteristics. *Neurosci Biobehav Rev* 2003; **27**(6)**:** 555-579.
53. Xu X, Holmes TC, Luo MH, Beier KT, Horwitz GD, Zhao F *et al.* Viral Vectors for Neural Circuit Mapping and Recent Advances in Trans-synaptic Anterograde Tracers. *Neuron* 2020; **107**(6)**:** 1029-1047.
54. Hoover WB, Vertes RP. Anatomical analysis of afferent projections to the medial prefrontal cortex in the rat. *Brain Struct Funct* 2007; **212**(2)**:** 149-179.
55. Dedic N, Kühne C, Jakovcevski M, Hartmann J, Genewsky AJ, Gomes KS *et al.* Chronic CRH depletion from GABAergic, long-range projection neurons in the extended amygdala reduces dopamine release and increases anxiety. *Nat Neurosci* 2018; **21**(6)**:** 803-807.
56. Sanford CA, Soden ME, Baird MA, Miller SM, Schulkin J, Palmiter RD *et al.* A Central Amygdala CRF Circuit Facilitates Learning about Weak Threats. *Neuron* 2017; **93**(1)**:** 164-178.
57. Chen W, Taché Y, Marvizón JC. Corticotropin-Releasing Factor in the Brain and Blocking Spinal Descending Signals Induce Hyperalgesia in the Latent Sensitization Model of Chronic Pain. *Neuroscience* 2018; **381:** 149-158.
58. Rouwette T, Klemann K, Gaszner B, Scheffer GJ, Roubos EW, Scheenen WJ *et al.* Differential responses of corticotropin-releasing factor and urocortin 1 to acute pain stress in the rat brain. *Neuroscience* 2011; **183:** 15-24.
59. Holland PR, Bartsch T. Involvement of corticotrophin-releasing factor and orexin-A in chronic migraine and medication overuse headache: findings from cerebrospinal fluid. *Cephalalgia* 2008; **28**(7)**:** 681-682.

60. Cabot PJ, Carter L, Gaiddon C, Zhang Q, Schäfer M, Loeffler JP *et al.* Immune cell-derived beta-endorphin. Production, release, and control of inflammatory pain in rats. *J Clin Invest* 1997; **100**(1)**:** 142-148.
61. Andreoli M, Marketkar T, Dimitrov E. Contribution of amygdala CRF neurons to chronic pain. *Exp Neurol* 2017; **298**(Pt A)**:** 1-12.
62. Mazzitelli M, Yakhnitsa V, Neugebauer B, Neugebauer V. Optogenetic manipulations of CeA-CRF neurons modulate pain- and anxiety-like behaviors in neuropathic pain and control rats. *Neuropharmacology* 2022; **210:** 109031.
63. Kita A, Imano K, Nakamura H. Involvement of corticotropin-releasing factor in the antinociception produced by interleukin-1 in mice. *Eur J Pharmacol* 1993; **237**(2-3)**:** 317-322.
64. Deussing JM, Chen A. The Corticotropin-Releasing Factor Family: Physiology of the Stress Response. *Physiological reviews* 2018; **98**(4)**:** 2225-2286.
65. Vita N, Laurent P, Lefort S, Chalon P, Lelias JM, Kaghad M *et al.* Primary structure and functional expression of mouse pituitary and human brain corticotrophin releasing factor receptors. *FEBS Lett* 1993; **335**(1)**:** 1-5.
66. Bale TL, Picetti R, Contarino A, Koob GF, Vale WW, Lee KF. Mice deficient for both corticotropin-releasing factor receptor 1 (CRFR1) and CRFR2 have an impaired stress response and display sexually dichotomous anxiety-like behavior. *J Neurosci* 2002; **22**(1)**:** 193-199.
67. Prouty EW, Waterhouse BD, Chandler DJ. Corticotropin releasing factor dose-dependently modulates excitatory synaptic transmission in the noradrenergic nucleus locus coeruleus. *The European journal of neuroscience* 2017; **45**(5)**:** 712-722.
68. Basbaum AI, Bautista DM, Scherrer G, Julius D. Cellular and molecular mechanisms of pain. *Cell* 2009; **139**(2)**:** 267-284.
69. Kuner R, Flor H. Structural plasticity and reorganisation in chronic pain. *Nat Rev Neurosci* 2016; **18**(1)**:** 20-30.
70. Latremoliere A, Woolf CJ. Central sensitization: a generator of pain hypersensitivity by central neural plasticity. *J Pain* 2009; **10**(9)**:** 895-926.
71. Neugebauer V, Mazzitelli M, Cragg B, Ji G, Navratilova E, Porreca F. Amygdala, neuropeptides, and chronic pain-related affective behaviors. *Neuropharmacology* 2020; **170:** 108052.
72. Lu VB, Biggs JE, Stebbing MJ, Balasubramanyan S, Todd KG, Lai AY *et al.* Brain-derived neurotrophic factor drives the changes in excitatory synaptic transmission in the rat superficial dorsal horn that follow sciatic nerve injury. *J Physiol* 2009; **587**(Pt 5)**:** 1013-1032.
73. Yang S, Chang MC. Chronic Pain: Structural and Functional Changes in Brain Structures and Associated Negative Affective States. *Int J Mol Sci* 2019; **20**(13).
74. Holahan MR, Kalin NH, Kelley AE. Microinfusion of corticotropin-releasing factor into the nucleus accumbens shell results in increased behavioral arousal and oral motor activity. *Psychopharmacology (Berl)* 1997; **130**(2)**:** 189-196.

75. Lemos JC, Shin JH, Alvarez VA. Striatal Cholinergic Interneurons Are a Novel Target of Corticotropin Releasing Factor. *J Neurosci* 2019; **39**(29)**:** 5647-5661.
76. Kono J, Konno K, Talukder AH, Fuse T, Abe M, Uchida K *et al.* Distribution of corticotropin-releasing factor neurons in the mouse brain: a study using corticotropin-releasing factor-modified yellow fluorescent protein knock-in mouse. *Brain Struct Funct* 2017; **222**(4)**:** 1705-1732.
77. Justice NJ, Yuan ZF, Sawchenko PE, Vale W. Type 1 corticotropin-releasing factor receptor expression reported in BAC transgenic mice: implications for reconciling ligand-receptor mismatch in the central corticotropin-releasing factor system. *J Comp Neurol* 2008; **511**(4)**:** 479-496.
78. Yao L, Rong Y, Ma X, Li H, Deng D, Chen Y *et al.* Extrasynaptic NMDA Receptors Bidirectionally Modulate Intrinsic Excitability of Inhibitory Neurons. *J Neurosci* 2022; **42**(15)**:** 3066-3079.
79. Pan G, Chen Z, Zheng H, Zhang Y, Xu H, Bu G *et al.* Compensatory Mechanisms Modulate the Neuronal Excitability in a Kainic Acid-Induced Epilepsy Mouse Model. *Front Neural Circuits* 2018; **12:** 48.
80. Huang YH, Lin Y, Brown TE, Han MH, Saal DB, Neve RL *et al.* CREB modulates the functional output of nucleus accumbens neurons: a critical role of N-methyl-D-aspartate glutamate receptor (NMDAR) receptors. *J Biol Chem* 2008; **283**(5)**:** 2751-2760.
81. Hu XT, White FJ. Glutamate receptor regulation of rat nucleus accumbens neurons in vivo. *Synapse* 1996; **23**(3)**:** 208-218.
82. Cooper DC, White FJ. L-type calcium channels modulate glutamate-driven bursting activity in the nucleus accumbens in vivo. *Brain Res* 2000; **880**(1-2)**:** 212-218.
83. Qi C, Guo B, Ren K, Yao H, Wang M, Sun T *et al.* Chronic inflammatory pain decreases the glutamate vesicles in presynaptic terminals of the nucleus accumbens. *Mol Pain* 2018; **14:** 1744806918781259.
84. Ziółkowska B. The Role of Mesostriatal Dopamine System and Corticostriatal Glutamatergic Transmission in Chronic Pain. *Brain Sci* 2021; **11**(10).
85. Zegers-Delgado J, Aguilera-Soza A, Calderón F, Davidson H, Verbel-Vergara D, Yarur HE *et al.* Type 1 Corticotropin-Releasing Factor Receptor Differentially Modulates Neurotransmitter Levels in the Nucleus Accumbens of Juvenile versus Adult Rats. *Int J Mol Sci* 2022; **23**(18).
86. Park BY, Lee JJ, Kim HJ, Woo CW, Park H. A neuroimaging marker for predicting longitudinal changes in pain intensity of subacute back pain based on large-scale brain network interactions. *Sci Rep* 2020; **10**(1)**:** 17392.
87. Löffler M, Levine SM, Usai K, Desch S, Kandić M, Nees F *et al.* Corticostriatal circuits in the transition to chronic back pain: The predictive role of reward learning. *Cell Rep Med* 2022; **3**(7)**:** 100677.
88. Baliki MN, Petre B, Torbey S, Herrmann KM, Huang L, Schnitzer TJ *et al.* Corticostriatal functional connectivity predicts transition to chronic back pain. *Nat Neurosci* 2012; **15**(8)**:** 1117-1119.
89. Waselus M, Van Bockstaele EJ. Co-localization of corticotropin-releasing factor and vesicular glutamate transporters within axon terminals of the rat dorsal raphe nucleus. *Brain Res* 2007; **1174:** 53-65.

90. Arrigoni E, Saper CB. What optogenetic stimulation is telling us (and failing to tell us) about fast neurotransmitters and neuromodulators in brain circuits for wake-sleep regulation. *Current opinion in neurobiology* 2014; **29:** 165-171.

91. Bartfai T, Iverfeldt K, Fisone G, Serfözö P. Regulation of the release of coexisting neurotransmitters. *Annu Rev Pharmacol Toxicol* 1988; **28:** 285-310.

Figures

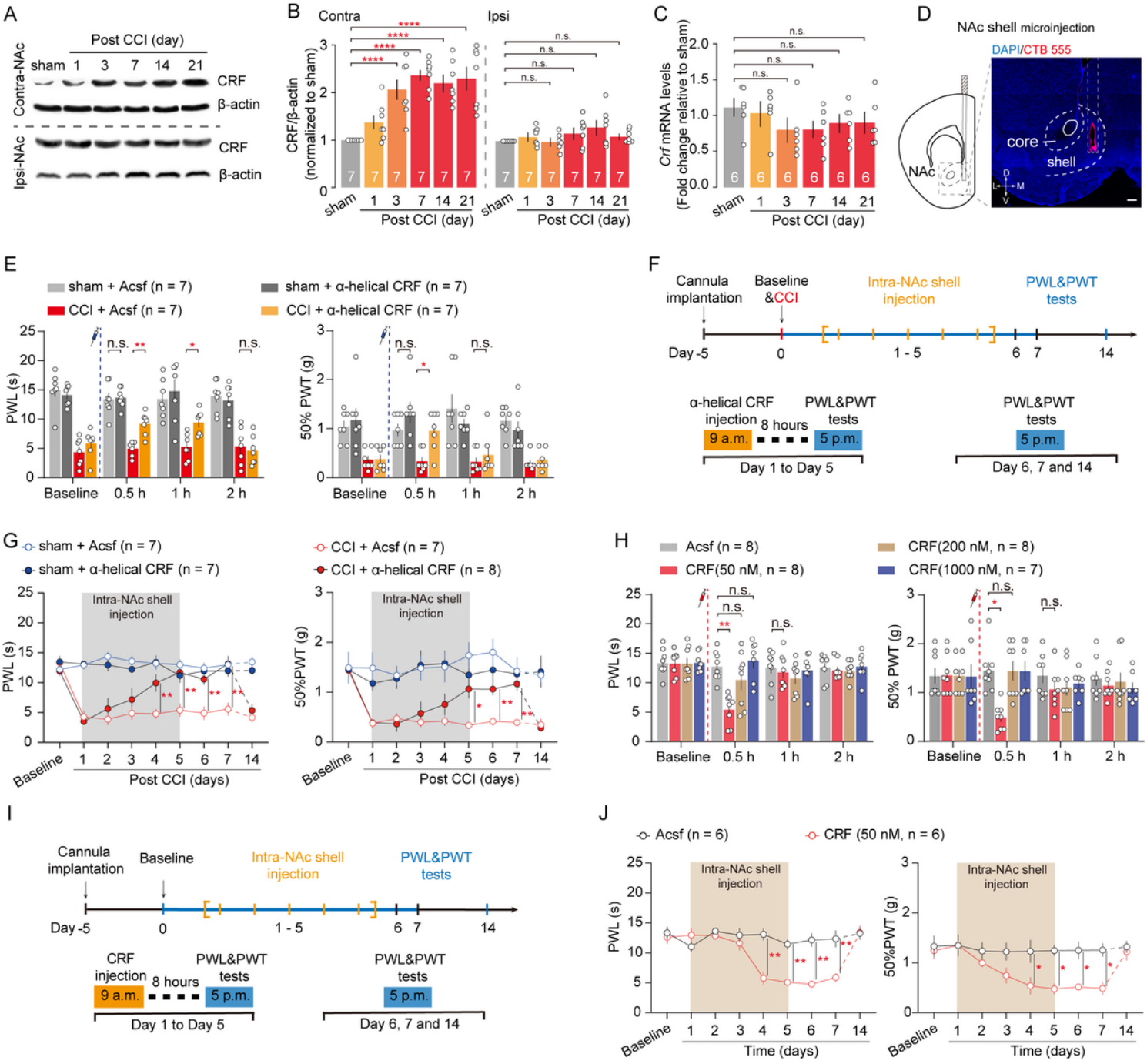

Figure 1

The NAcS CRF signaling regulates pain sensation. A Representative band showing ipsilateral and contralateral NAc CRF protein expression in sham control mice and CCI mice on days 1, 3, 7, 14, and 21 following the CCI surgery. **B** Quantitative data showing NAc CRF protein expression in sham and CCI groups on days 1, 3, 7, 14, and 21 following the CCI surgery. n = 7 mice/group. Contra: group, $F_{(5, 36)}$ = 10.96, p < 0.0001; Sham versus CCI day 3 p = 0.0004; day 7 p < 0.0001; day 14 p < 0.0001; day 21 p < 0.0001. Ipsi: group, $F_{(5, 36)}$ = 1.519, p = 0.2084. **C** Quantitative data showing contralateral NAc *Crf* mRNA level in sham and CCI groups on days 1, 3, 7, 14, and 21 following the CCI surgery. n = 6 mice/group. Group, $F_{(5, 30)}$ = 0.8912, p = 0.4994. **D** Schematic and histological verification of microinjection sites of the NAcS. Scale bar, 200 μm. **E** Intra-NAcS microinjection of -helical CRF before behavioral tests on day 7 after CCI surgery increased PWLs (*left*) and 50%PWTs (*right*) in CCI-affected hind paws. n = 7 mice/group. PWL: group, $F_{(3, 24)}$ = 58.38, p < 0.0001; CCI + Acsf versus CCI + -helical CRF, 0.5h p = 0.0026, 1h p = 0.0166. 50%PWTs: group, $F_{(3, 24)}$ = 34.95, p < 0.0001; CCI + Acsf versus CCI + -helical CRF, 0.5h p = 0.0229. **F** Experimental timeline. The -helical CRF was microinjected to NAcS daily for 5 days after CCI surgery. PWLs and 50%PWTs were assessed at 8 hours after intra-NAcS injection. **G** Daily injection of -helical CRF to NAcS increased the PWLs (*left*) and 50%PWTs (*right)* in CCI mice, and the effect can persist for 2 days after the injection is terminated. n = 7 - 8 mice/group. PWL: group, $F_{(3, 25)}$ = 89.17, p < 0.0001; CCI + Acsf versus CCI + -helical CRF, 4d p = 0.0421, 5d p = 0.0431, 6d p = 0.0098, 7d p = 0.0027. 50%PWT: group, $F_{(3, 25)}$ = 23.46, p < 0.0001; CCI + Acsf versus CCI + -helical CRF, 5d p = 0.0196, 6d p = 0.0049, 7d p = 0.0034. **H** Intra-NAcS microinjection of CRF decreased PWLs (*left*) and 50%PWTs (*right*) in naïve mice. n = 7 - 8 mice/group. PWL: group, $F_{(3, 27)}$ = 4.377, p = 0.0123; Acsf versus CRF 50nM, 0.5h p = 0.0013. 50%PWTs: group, $F_{(3, 27)}$ = 2.561, p = 0.0758; Acsf versus CRF 50nM, 0.5h p = 0.0486. **I** Experimental timeline. The CRF was microinjected into the NAcS daily for 5 days. PWLs and PWTs were assessed at 8 hours after intra-NAcS injection. **J** Daily injection of CRF to NAcS can decrease the PWLs (*left*) and 50%PWTs (*right)* in naïve mice, and the effect can persist for 2 days after the injection is terminated. n = 6 mice/group. PWL: group, $F_{(1, 10)}$ = 44.07, p < 0.0001; Acsf versus CRF, 4d p < 0.0001, 5d p = 0.0001, 6d p < 0.0001, 7d p < 0.0001. 50%PWT: group, $F_{(1, 10)}$ = 28.23, p = 0.0003; Acsf versus CRF, 5d p = 0.0398, 6d p = 0.0421, 7d p = 0.0409. *p < 0.05; **p < 0.01; ***p < 0.001; ****p < 0.0001. Data was analyzed by (**B, C**) one-way ANOVA followed by *Bonferroni's* test for multiple comparisons, or (**E, G, H, J**) two-way ANOVA followed by *Bonferroni's* test for multiple comparisons. Error bars indicate SEM. Acsf, artificial cerebrospinal fluid; CTB, Cholera Toxin Subunit B; NAc, nucleus accumbens; NAcS, nucleus accumbens shell; Contra, contralateral; Ipsi, Ipsilateral.

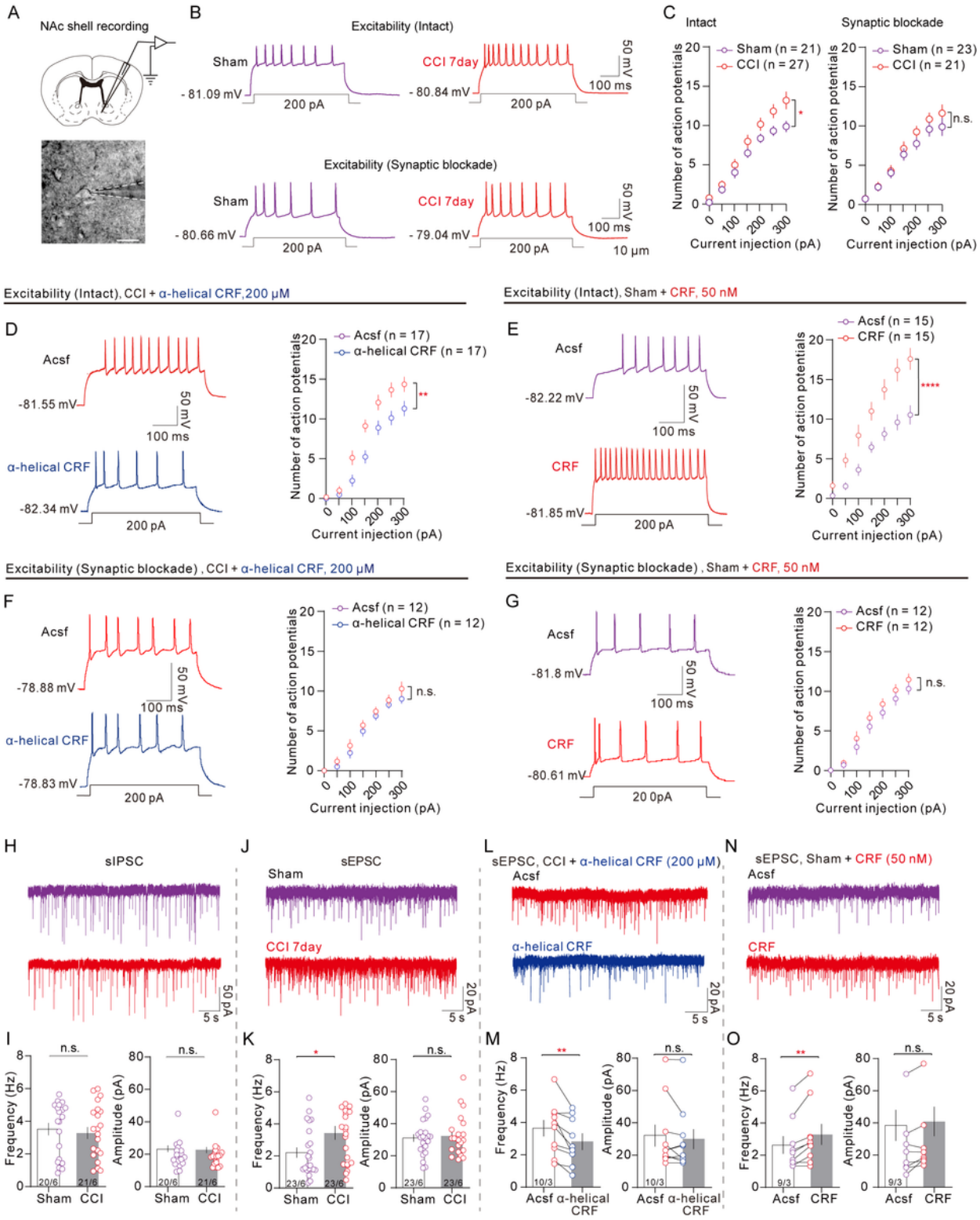

Figure 2

CRF enhances excitatory synaptic transmission and neuronal excitability in the NAcS. **A** Schematic and a typical image of electrophysiological recording in NAcS on day 7 after the sham or CCI surgery. Scale bar, 10 μm. **B** Sample of whole-cell patch-clamp recording of eAPs in NAcS neurons from sham and CCI groups with synaptic transmission intact (*top*) or synaptic transmission blocked (*bottom*). **C** Quantitative data showing the number of eAPs of NAcS neurons in sham and CCI mice. (*left*) With synaptic

transmission intact, the numbers of eAPs of NAcS neurons were increased in CCI mice. n_{sham} = 21 cells from 6 mice, n_{CCI} = 27 cells from 6 mice. Group, $F_{(1, 46)}$ = 4.744, p = 0.0346. (*right*) With fast synaptic transmission blocked, eAPs of NAcS neurons showed no significant change in CCI mice. n_{sham} = 23 cells from 6 mice, n_{CCI} = 21 cells from 6 mice. Group, $F_{(1, 42)}$ = 1.152, p = 0.2892. **D** Sample traces and the quantitative data for whole-cell patch-clamp recording of eAPs of NAcS neurons in CCI mice. (*left*) Sample trace of NAcS neurons in response to a 200-pA depolarizing current step before (Acsf, red) and after -helical CRF (200 μM, blue) application. (*right*) In CCI mice, -helical CRF perfusion decreased the numbers of eAPs of NAcS neurons. n = 17 cells from 6 mice. Group, $F_{(1, 32)}$ = 10.53, p = 0.0028. **E** Sample traces and the quantitative data for whole-cell patch-clamp recording of eAPs of NAcS neurons. (*left*) Sample recordings of eAPs of NAcS neurons in response to a 200-pA depolarizing current step before (Acsf, purple) and after CRF (50 nM, red) application. (*right*) In sham mice, CRF perfusion increased the numbers of eAPs of NAcS neurons. n = 15 cells from 5 mice. Group, $F_{(1, 28)}$ = 15.81, p = 0.0004. **F** Sample traces and the quantitative data for eAPs of NAcS neurons in CCI mice with synaptic transmission blocked. (*left*) Sample recordings of eAPs of NAcS neurons in response to a 200-pA depolarizing current step before (Acsf, red) and after -helical CRF (200 μM, blue) application. (*right*) In CCI mice, -helical CRF perfusion decreased the numbers of eAPs of NAcS neurons. n = 12 cells from 4 mice. Group, $F_{(1, 22)}$ = 1.263, p = 0.2732. **G** Sample traces and the quantitative data for whole-cell patch-clamp recording of eAPs of NAcS neurons in sham mice with synaptic transmission blocked. (*left*) Sample recordings of eAPs of NAcS neurons in response to a 200-pA depolarizing current step before (Acsf, purple) and after CRF (50 nM, red) application. (*right*) In sham mice, CRF perfusion increased the numbers of eAPs of NAcS neurons. n = 12 cells from 4 mice. Group, $F_{(1, 22)}$ = 0.8817, p = 0.3579. **H** Example recordings of sIPSC in NAcS neurons from sham and CCI mice. **I** Compared with sham group, CCI mice did show no significant difference in the sIPSC frequency (*left*) and amplitude (*right*) of neurons in NAcS. n_{sham} = 20 cells from 6 mice, n_{CCI} = 21 cells from 6 mice. Frequency: $t_{(39)}$ = 0.3887, p = 0.6996. Amplitude: $t_{(39)}$ = 0.1057, p = 0.9163. **J** Example recordings of sEPSC in NAcS neurons from sham and CCI mice. **K** Compared with sham group, CCI mice showed increased frequency (*left*), but not amplitude (*right*) of sEPSC of neurons in NAcS. n_{sham} = 23 cells from 6 mice, n_{CCI} = 23 cells from 6 mice. Frequency: $t_{(44)}$ = 2.304, p = 0.026. Amplitude: $t_{(44)}$ = 0.9505, p = 0.347. **L** Example recordings of sEPSCs from NAcS neurons before and after perfusion of -helical CRF in CCI mice. **M** In CCI mice, -helical CRF perfusion decreased the frequency (*left*), but not amplitude (*right*) of sEPSCs in NAcS neurons. n = 10 cells from 3 mice. Frequency: $t_{(9)}$ = 3.58, p = 0.0059. Amplitude: $t_{(9)}$ = 1.246, p = 0.2444. **N** Example recordings of sEPSCs from NAcS neurons before and after perfusion of CRF in sham mice. **O** In sham mice, CRF perfusion increased the frequency (*left*), but not the amplitude (*right*) of sEPSCs in NAcS neurons. n = 9 cells from 3 mice. Frequency: $t_{(8)}$ = 3.878, p = 0.0047. Amplitude: $t_{(8)}$ = 1.847, p = 0.1019. *p < 0.05; **p < 0.01, ***p < 0.001, ****p < 0.0001. Error bars indicate SEM. Data was analyzed by (**C, D, E, F, G**) two-way ANOVA followed by *Bonferroni's* test for multiple comparisons, (**E, G**) unpaired *t* test for two group comparisons, or (**I, K**) paired *t* test. Acsf, artificial cerebrospinal fluid; NAcS, nucleus accumbens shell; eAPs, evoked action potentials by depolarizing current injections; sIPSC, spontaneous inhibitory postsynaptic currents; sEPSC, spontaneous excitatory postsynaptic currents.

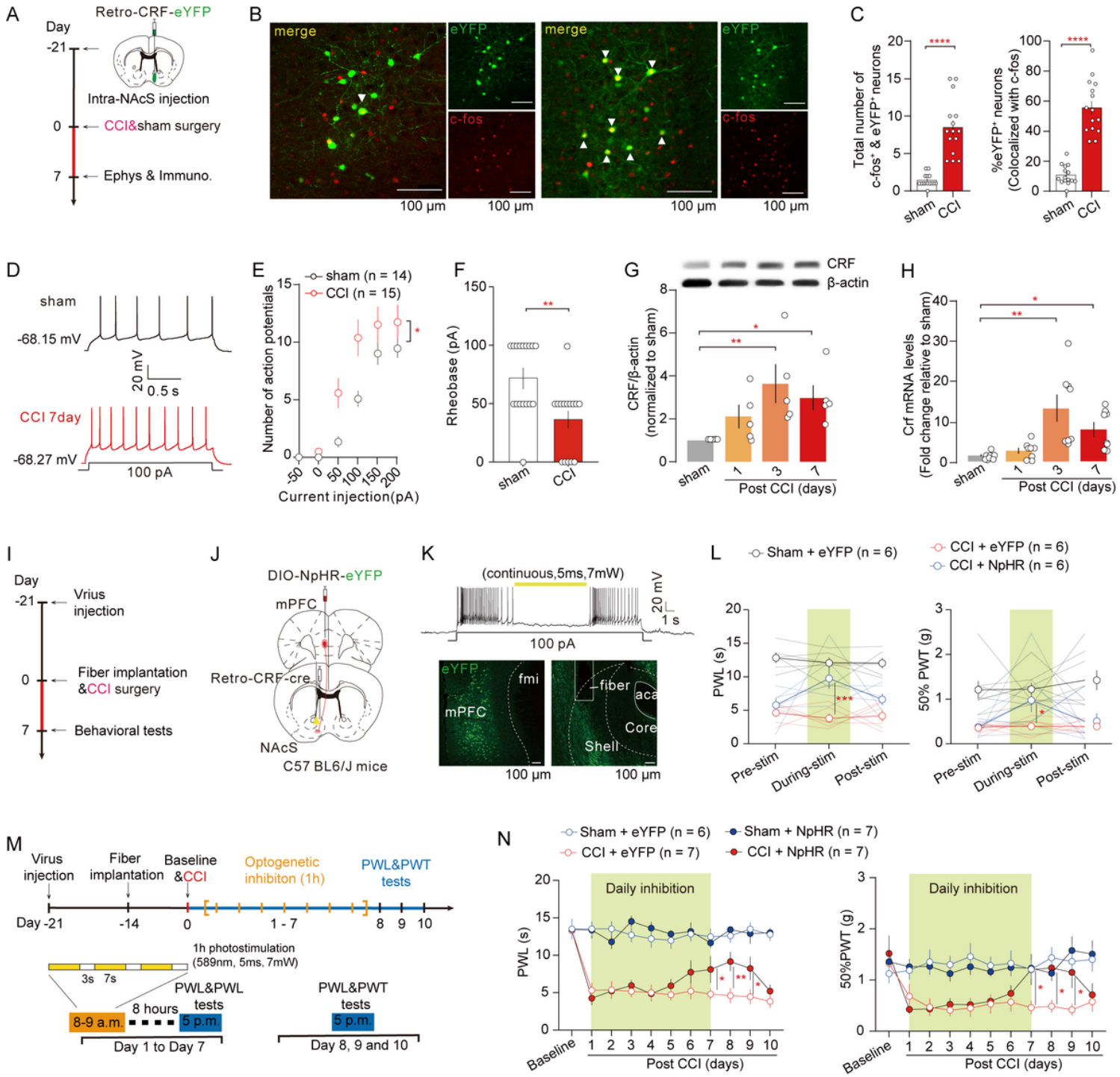

Figure 3

mPFC^{CRF}→NAcS circuit is required for CCI-induced hyperalgesia. A Experimental timeline. Electrophysiological recordings and immunofluorescence were executed on day 7 after the sham or CCI surgery. **B** Representative confocal images for c-Fos-positive neurons in mPFC^{CRF}→NAcS circuit from sham and CCI mice. White arrows indicate co-labeled neurons. Scale bars, 100 μm. **C** Quantitative data showing that CCI increased c-Fos expression in mPFC^{CRF}→NAcS neurons. (*left*) Total numbers of mPFC neurons co-expressing the eYFP and c-Fos. n = 15 slices from 5 mice/group. Sham, 1.4 ± 0.2138; CCI, 8.533 ± 0.9704. $t_{(15.36)}$ = 7.179, p < 0.0001. (*right*) Percentages of c-Fos-expressing neurons in eYFP-

labeled mPFC neurons. Sham, 10.77 ± 1.656; CCI, 55.95 ± 4.609. $t_{(17.55)} = 9.227$, $p < 0.0001$. **D** Sample of eAPs of $mPFC^{CRF}$→NAcS circuit neurons in response to a 100-pA depolarizing current step in sham (black) and CCI (red) mice. **E** Quantitative data shows that neurons of $mPFC^{CRF}$→NAcS circuit in CCI mice exhibited increased numbers of eAPs. $n_{sham} = 14$ cells from 4 mice, $n_{CCI} = 15$ cells from 5 mice. Group, $F_{(1, 26)} = 6.627$, $p = 0.0161$. **F** Quantitative data shows that neurons of $mPFC^{CRF}$→NAcS circuit in CCI mice had a lower rheobase current. $n_{sham} = 14$ cells from 4 mice, $n_{CCI} = 15$ cells from 5 mice. $p = 0.006$, *Mann Whitney* test. **G** Representative bands and quantitative data showing contralateral mPFC CRF protein expression in sham control mice and CCI mice on days 1, 3, and 7 following the CCI surgery. $n =$ 5 mice/group. Summary, $p = 0.021$, Sham versus Day 3, $p = 0.0181$, Sham versus Day 7, $p = 0.0249$, *Kruskal Wallis* test. **H** Contralateral mPFC CRF mRNA expression in sham and CCI mice on day 1, 3, 7 after CCI surgery. $n =$ 8 mice/group. Summary, $p = 0.0041$, Sham versus Day 3, $p = 0.0363$, Sham versus Day 7, $p = 0.0076$, *Kruskal Wallis* test. **I** Experimental timeline. **J** Schematic of the virus injection for optogenetic inhibition of $mPFC^{CRF}$→NAcS circuit neurons. **K** (*top*) Optical stimulation in a $mPFC^{CRF}$→NAcS CRF-containing neuron with yellow light (589 nm, yellow bar) inhibited action potentials induced by the injection of depolarizing current. (*bottom*) Typical confocal image showing the eYFP expression in the mPFC and NAcS. **L** Acute real-time optogenetic inhibition of the $mPFC^{CRF}$→NAcS circuit in the NAcS increased PWLs and 50%PWTs in CCI mice. PWLs: $n =$ 6 mice/group. Group, $F_{(2, 15)} = 134.6$, $p < 0.0001$; CCI + eYFP versus CCI + NpHR, During-stim $p = 0.0001$. 50%PWTs: $n =$ 8 mice/group. Group, $F_{(2, 21)} = 44.65$, $p < 0.0001$; CCI + eYFP versus CCI + NpHR, During-stim $p = 0.0275$. **M** Experimental timeline. The 1-hour optogenetic inhibition of $mPFC^{CRF}$→NAcS circuit was executed daily for seven days after CCI surgery. PWLs and 50%PWTs were assessed at 8 hours after inhibition. **N** Statistics showing repeated optogenetic inhibition of $mPFC^{CRF}$→NAcS circuit increased the PWLs and 50%PWTs of CCI mice. PWLs: $n =$ 6 - 7 mice/group. Group, $F_{(3, 22)} = 103.6$, $p < 0.0001$; CCI + eYFP versus CCI +NpHR, 8d $p = 0.009$, 9d $p = 0.0443$. 50%PWT: $n =$ 6 - 7 mice/group. Group, $F_{(3, 22)} = 8.33$, $p = 0.0007$; CCI + eYFP versus CCI +NpHR, 7d $p = 0.0447$ 8d $p = 0.0421$, 9d $p = 0.0495$. $^{**}p < 0.01$, $^{***}p < 0.001$, $^{****}p < 0.001$. Error bars indicate SEM. Data was analyzed by (**E, L, N**) two-way ANOVA followed by *Bonferroni's* test for multiple comparisons, (**C**) unpaired *t* test for two group comparisons, (**F**) *Mann Whitney* test, or (**G, H**) *Kruskal Wallis* test. NAcS, nucleus accumbens shell; mPFC, medial prefrontal cortex; eAPs, evoked action potentials by depolarizing current injections.

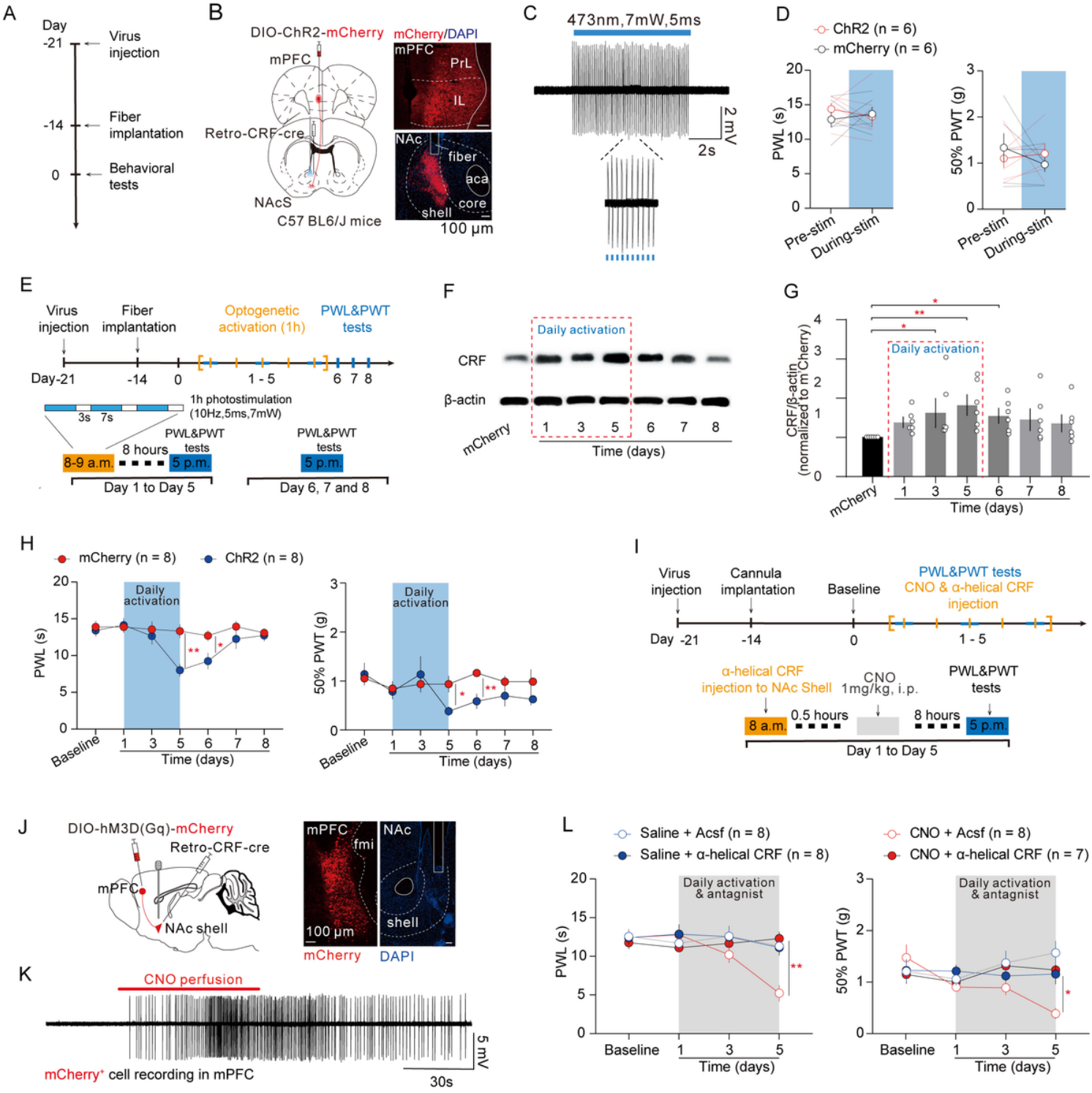

Figure 4

The sufficient role of the mPFC^{CRF}→NAcS circuit in pain sensation regulation. A Experimental timeline. **B** Schematic of the virus injection for optogenetic activation of mPFC^{CRF}→NAcS circuit and a typical confocal image showing the mCherry expression in mPFC^{CRF}→NAcS neurons contralateral to the CCI hindpaw. **C** Optical stimulation in with blue light (473 nm, blue bar) reliably induced APs in the mPFC^{CRF}→NAcS circuit neurons. **D** Acute real-time optogenetic activation of the mPFC^{CRF}→NAcS circuit in the NAc did not influence the PWLs (*left*) and 50%PWTs (*right*) in naïve mice. PWL: *n* = 6 mice/group.

Group, $F_{(1, 10)}$ = 0.2053, p =0.6602; CCI + mCherry versus CCI + ChR2, During-stim p = 0.9705. PWT: n = 6 mice/group. Group, $F_{(1, 10)}$ = 0.4172, p = 0.5329; CCI + mCherry versus CCI + ChR2, During-stim p = 0.9411. **E** Experimental timeline. The 1-hour optogenetic activation of mPFC^{CRF}→NAcS circuit was executed daily for five days. PWLs and 50%PWTs were assessed at 8 hours after the termination of activation. **F** Representative bands showing ipsilateral NAc CRF protein expression in the mCherry group and ChR2 group on days 1, 3, 5, 6, 7, and 8 following the first activation. **G** Quantitative data shows that repeated optogenetic activation increased the CRF protein level in NAc. n = 6 mice/group. Summary, p = 0.0303, mCherry versus Day 1, p = 0.1107, mCherry versus Day 3, p = 0.0376, mCherry versus Day 5, p = 0.0049, mCherry versus Day 6, p = 0.0376, *Kruskal Wallis* test. **H** Statistics show that repeated optogenetic activation of mPFC^{CRF}→NAcS circuit can decrease the PWLs (*left*) and 50%PWTs (*right*) of naïve mice, and the effect can persist for 1 day after the manipulation is terminated. PWL: n = 8 mice/group. Group, $F_{(1, 14)}$ = 11.44, p = 0.0045; mCherry versus ChR2, 5d p = 0.0007, 6d p = 0.048. 50%PWT: n = 8 mice/group. Group, $F_{(1, 14)}$ = 4.561, p = 0.0509; mCherry versus ChR2, 5d p = 0.0168, 6d p = 0.0079. **I** Experimental timeline. The chemogenetic activation of the mPFC^{CRF}→NAcS circuit and the intra-NAcS injection of -helical CRF was executed daily for five days. PWLs and 50%PWTs were assessed at 8 hours after CNO injection. **J** Schematic of the virus injection for chemogenetic activation of mPFC^{CRF}→NAcS circuit, and typical confocal image showing the expression of mCherry in mPFC and the cannula implanted to NAcS. **K** Sample traces from mPFC slice showing that the firing of mPFC^{CRF}→NAcS neurons is increased by CNO perfusion. **L** Statistics show that intra-NAcS injection of -helical CRF reversed hyperpathia induced by repeated activation of mPFC^{CRF}→NAcS circuit. (*left*) PWL: n = 7 - 8 mice/group. Group, $F_{(3, 27)}$ = 1.88, p = 0.1568; Gq + Acsf versus ChR2 + -helical CRF, 5d p = 0.0017. (right) 50%PWT: n = 7 - 8 mice/group. Group, $F_{(3, 27)}$ = 3.162, p = 0.0407; ChR2 + Acsf versus Gq + -helical CRF, 5d p = 0.0455. *p < 0.05; **p < 0.01. Error bars indicate SEM. Data was analyzed by (**D, H, L**) two-way ANOVA followed by *Bonferroni's* test for multiple comparisons, or (**G**) *Kruskal Wallis* test. NAcS, nucleus accumbens shell; mPFC, medial prefrontal cortex.

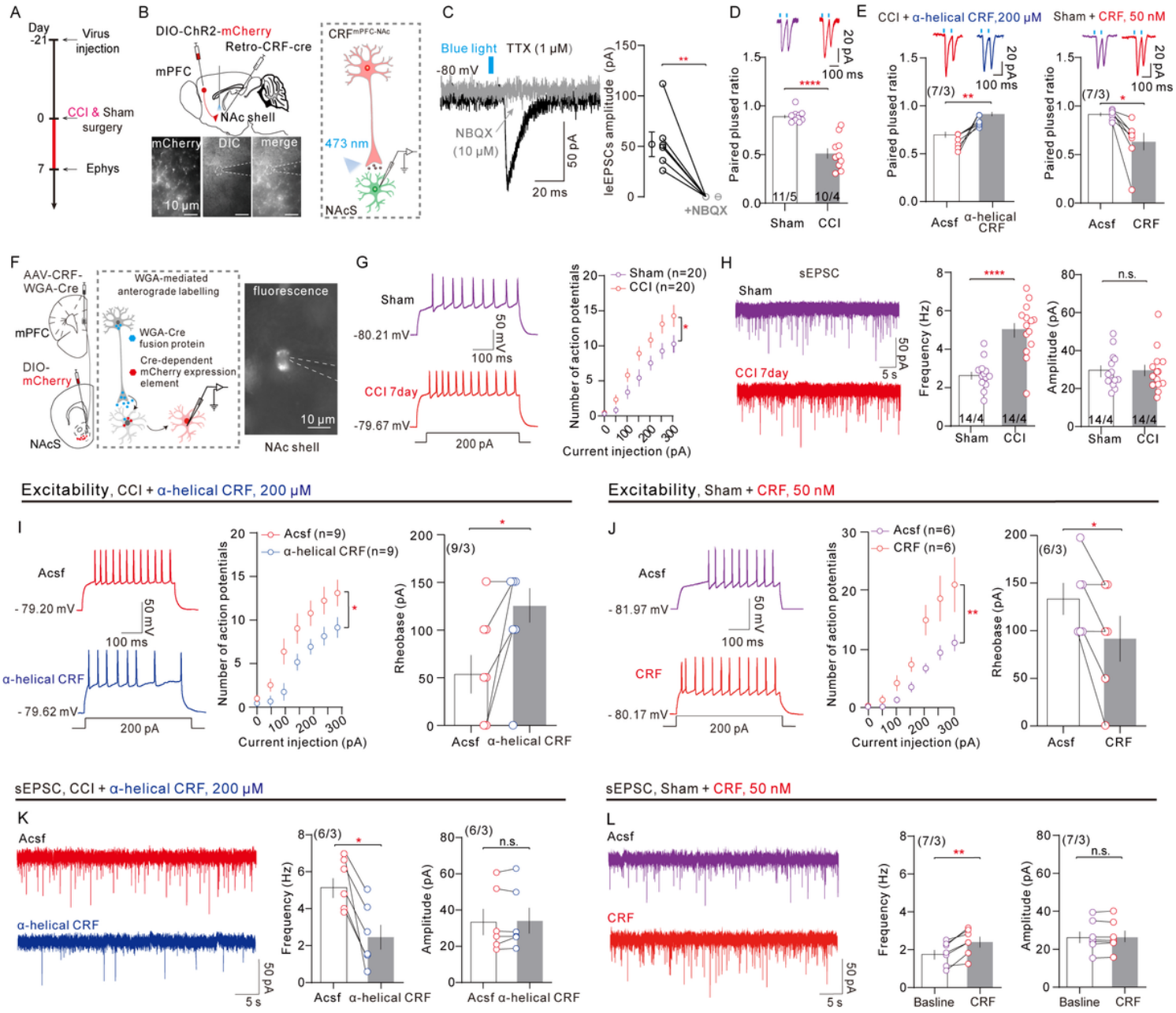

Figure 5

Identifying monosynaptic connection in the mPFC^{CRF}→NAcS circuit and its functional alteration in chronic neuropathic pain. **A** Experimental timeline. **B** (*left*) Schematic of the virus injection for optogenetic activation of mPFC^{CRF}→NAcS circuit and typical micrograph showing the electrophysiological recording of NAcS-receiving neurons (*right*) Schematic of the in vitro electrophysiological recording for light-evoked excitatory postsynaptic currents (leEPSCs) and paired-pulse ratio (PPR) in NAcS-receiving neurons. **C** (*left*) Optical activation of terminals of mPFC^{CRF}→NAcS circuit with blue light evoked with blue light–evoked glutamatergic monosynaptic, AMPARs-mediated EPSCs. (*right*) The AMPA receptor antagonist NBQX blocked leEPSCs in the NAcS neurons. n_{CCI} = 6 cells, $t_{(5)}$ = 4.512, p = 0.0063. **D** Quantitative results showing that the PPR of NAcS-receiving neurons was decreased in the CCI group. n_{sham} = 11 cells from 5 mice, n_{CCI} = 10 cells from 4 mice. $t_{(19)}$ = 7.038, p <

0.0001. **E** *(left)* Quantitative results showing that -helical CRF perfusion increased the PPR of NAcS-receiving neurons in CCI mice. n = 7 cells from 3 mice. $t_{(6)}$ = 4.368, p = 0.0047. *(right)* Quantitative results showing that CRF perfusion decreased the PPR of NAcS-receiving neurons in sham mice. n = 7 cells from 3 mice. $t_{(6)}$ = 3.622, p = 0.0111. **F** *(left)* Schematic of the virus injection and the WGA-medicated transsynaptic transmission. *(right)* Typical micrograph showing the electrophysiological recording of mCherry-labeled NAcS-receiving neurons. **G** *(left)* Sample of whole-cell patch-clamp recording of eAPs of mCherry-labeled NAcS neurons in sham (purple) and CCI (red) mice. *(right)* Quantitative data showing that the numbers of eAPs in mCherry-labeled NAcS neurons were increased in CCI mice. n_{sham} = 20 cells from 5 mice, n_{CCI} = 20 cells from 5 mice. Group, $F_{(1, 38)}$ = 7.578, p = 0.009. **H** *(left)* Example recordings of sEPSC in mCherry-labeled NAcS neurons from sham and CCI mice. Compared with sham group, CCI mice showed increased frequency (*middle)*, but not amplitude (*right*) of sEPSC of mCherry-labeled neurons in NAcS. n_{sham} = 14 cells from 4 mice, n_{CCI} = 14 cells from 4 mice. Frequency: $t_{(26)}$ = 5.568, p < 0.0001. Amplitude: $t_{(26)}$ = 0.0003, p = 0.9998. **I** Sample traces and the quantitative data for whole-cell patch-clamp recording of eAPs of mCherry-labeled NAcS neurons in CCI mice. (*left*) Sample recordings of eAPs of mCherry-labeled NAcS neurons in response to a 200-pA depolarizing current step before (Acsf, red) and after -helical CRF (200 μM, blue) application. (*middle*) In CCI mice, -helical CRF perfusion increased the numbers of eAPs of mCherry-labeled neurons. n = 9 cells from 3 mice. Group, $F_{(1, 16)}$ = 6.181, p = 0.0243. (*right*) Minimal voltage threshold to induce eAPs was higher after -helical CRF perfusion. n = 9 cells from 3 mice. *Summary*, p = 0.0156, *Wilcoxon* test. **J** Sample traces and the quantitative data for whole-cell patch-clamp recording of eAPs of mCherry-labeled NAcS neurons in sham mice. (*left*) Sample recordings of eAPs of mCherry-labeled NAcS neurons in response to a 200-pA depolarizing current step before (Acsf, purple) and after CRF (50 nM, red) application in sham mice. (*middle*) In sham mice, CRF perfusion increased the numbers of eAPs of mCherry-labeled neurons. n = 6 cells from 3 mice. Group, $F_{(1, 10)}$ = 12.19, p = 0.0058. (*right*) Minimal voltage threshold to induce eAPs was lower after CRF perfusion. n = 6 cells from 3 mice. *Summary*, p = 0.0457, *Wilcoxon* test. **K** In CCI mice, -helical CRF perfusion decreased the frequency, but not amplitude of sEPSCs in mCherry-labeled NAcS neurons. (*left*) Example recordings of sEPSCs from mCherry-labeled NAcS neurons before and after perfusion of -helical CRF in CCI mice. (*middle*) -helical CRF perfusion decreased the frequency of sEPSCs in mCherry-labeled NAcS neurons. n = 6 cells from 3 mice. $t_{(5)}$ = 4.314, p = 0.0076. (*right*) -helical CRF perfusion did not influence the sEPSCs amplitudes in mCherry-labeled NAcS neurons. n = 6 cells from 3 mice. $t_{(5)}$ = 0.8738, p = 0.4222. **L** In sham mice, CRF perfusion increased the frequency, but not amplitude of sEPSCs in mCherry-labeled NAcS neurons. (*left*) Example recordings of sEPSCs from mCherry-labeled NAcS neurons before and after perfusion of CRF in sham mice. (*middle*) CRF perfusion increased the frequency of sEPSCs in mCherry-labeled NAcS neurons. n = 7 cells from 3 mice. $t_{(6)}$ = 5.263, p = 0.0019. (*right*) CRF perfusion did not influence the sEPSCs amplitudes in mCherry-labeled NAcS neurons. n = 7 cells from 3 mice. $t_{(6)}$ = 3.622, p = 0.0111. *p < 0.05; **p < 0.01, ***p < 0.001, ****p < 0.0001. Error bars indicate SEM. Data was analyzed by (**E, P, Q**) two-way ANOVA followed by *Bonferroni's* test for multiple comparisons, (**P, Q**) *Wilcoxon* test, (**H, K**) unpaired *t* test for two group comparisons, or (**I, M, N, O**) paired *t* test. Acsf, artificial cerebrospinal fluid; NAcS, nucleus accumbens shell; eAPs, evoked action potentials by depolarizing

current injections; mPFC, medial prefrontal cortex; PPR, paired-pulse ratio; sEPSC, spontaneous excitatory postsynaptic currents.

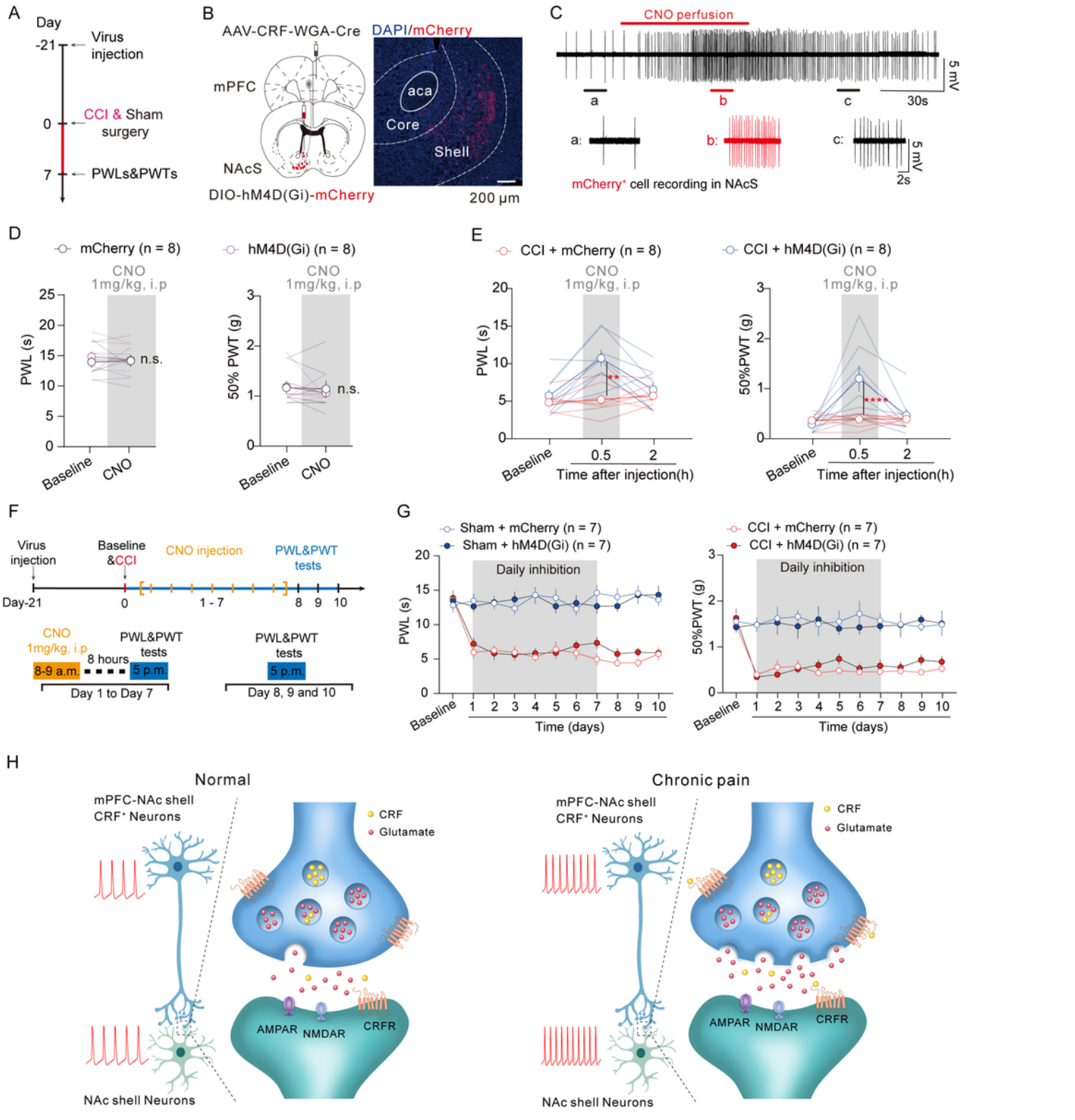

Figure 6

The role of NAcS-receiving neurons innervated by mPFC CRF-containing neurons in pain sensation regulation. A Experimental timeline. **B** Schematic of the virus injection and typical confocal image

showing the expression of mCherry in the NAcS-receiving neurons. **C** Sample traces and from NAcS slices showing that the firing activity of the NAcS-receiving neurons are inhibited by CNO perfusion. **D** Acute chemogenetic inhibition of the NAcS-receiving neurons did not influence the PWLs (*left*) and 50%PWTs (*right*) in naïve mice. PWL: n = 8 mice/group. Group, $F_{(1, 14)} = 0.2223$, $p = 0.6445$; mCherry versus Gi, CNO $p = 0.9901$. 50%PWTs: group, $F_{(1, 14)} = 0.048$, $p = 0.8299$; mCherry versus Gi, CNO $p = 0.8753$. **E** Single chemogenetic inhibition of the NAcS-receiving neurons increased PWLs (*left*) and 50%PWTs (*right*) in CCI mice. PWL: n = 8 mice/group. Group, $F_{(1, 6)} = 4.964$, $p = 0.0674$; mCherry versus Gi, CNO $p < 0.0001$. 50%PWTs: n = 8 mice/group. Group, $F_{(1, 6)} = 6.579$, $p = 0.0428$; mCherry versus Gi, CNO $p = 0.0443$. **F** Experimental timeline. Chemogenetic inhibition of the NAcS-receiving neurons was executed daily for seven days. PWLs and 50%PWTs were assessed at 8 hours after CNO injection. **G** Statistics showing that repeated inhibition of the NAcS-receiving neurons did not influence the PWLs (*left*) and 50%PWTs (*right*) of CCI mice. PWL: n = 7 mice/group. Group, $F_{(3, 24)} = 41.36$, $p < 0.0001$; mCherry + CCI versus Gi + CCI, 6d $p = 0.8448$, 7d $p = 0.2916$, 8d $p = 0.7535$, 9d $p = 0.6720$. 50%PWTs: n = 7 mice/group. Group, $F_{(3, 24)} = 113.5$, $p < 0.0001$; mCherry + CCI versus Gi + CCI, 6d $p = 0.9878$, 7d $p = 0.9444$, 8d $p = 0.9878$, 9d $p = 0.6497$. **H** Schematic summary of the main findings illustrating that increased CRF release in the $mPFC^{CRF} \rightarrow$NAcS circuit contributed to the persistent pain state. *$p < 0.05$; **$p < 0.01$, ***$p < 0.001$, ****$p < 0.0001$. Error bars indicate SEM. Data was analyzed by (**D, E, G**) two-way ANOVA followed by *Bonferroni's* test for multiple comparisons. NAcS, nucleus accumbens shell; mPFC, medial prefrontal cortex; AMPAR, α-amino-3-hydroxy-5-methyl-4-isoxazole-propionic acid receptor; NMDAR, N-methyl-D-aspartate receptor.

Supplementary Files

This is a list of supplementary files associated with this preprint. Click to download.

- Supplementalinformation.docx